JOURNAL

ENGINEERING MECHANICS DIVISION

Proceedings of the American Society of Civil Engineers

CONTENTS

January, 1956

Papers
(Discussion open until May 1, 1956)

Paper | Page

863 Vibrations of Beams on Many Supports
by John W. Miles 863-1

870 On the Deflections of Bow Girders of Non-Circular Shapes
by Enrico Volterra 870-1

Discussion

876 Contents i

JOURNAL
ENGINEERING MECHANICS DIVISION
Proceedings of the American Society of Civil Engineers

VIBRATIONS OF BEAMS ON MANY SUPPORTS

John W. Miles*
(Proc. Paper 863)

SUMMARY

The natural frequencies of a continuous beam resting on an arbitrary number of uniformly spaced supports are determined from a difference equation formulation. These frequencies fall in periodically spaced groups that are separated by spectral gaps of widths equal to approximately half the interval between the natural frequencies of a single beam on a square root frequency scale. These groups tend to uniform spectra as the number of supports tends to infinity, but the gaps remain, giving a band-pass character to the entire spectrum. Wave propagation along an infinite, periodically supported beam is discussed and the phase and group velocities evaluated as functions of frequency.

INTRODUCTION

The natural frequencies of continuous beams on several, uniformly spaced supports have been determined by Ayre and Jacobsen,(1) their results being presented in the form on a nomograph. The purpose of the present paper is to present an analytical solution, which offers certain advantages, especially when the number of supports is large. The limiting case of an infinite beam on periodically spaced supports is of particular interest, both because of the band-pass character of its spectrum and because it has been suggested as a model for the study of flutter of periodically supported aircraft structures,(2) albeit without recognition of the nature of the resulting spectrum.

We remark that both the problem and the method of solution considered here** find their natural antecedants in Brooks Taylor's classical study (1713) of a massless, elastic string carrying equally spaced, point masses.(3) The

Note: Discussion open until May 1, 1956. Paper 863 is part of the copyrighted Journal of the Engineering Mechanics Division of the American Society of Civil Engineers, Vol. 82 No. EM 1, January, 1956.

* Prof. of Eng., Univ. of California, Los Angeles, Calif.

** The application of finite difference methods to beam loading problems is, of course, well known; see, e.g., Th. v. Karman and M. Biot, Mathematical Methods in Engineering (McGraw-Hill, New York, 1940), p. 442.

analysis of such systems was further extended by Rayleigh[4,5] in order to generalize the wave propagation phenomena suggested by Reynolds' disconnected pendulums and the mechanical models of atomic radiation suggested by Fitzgerald (although Rayleigh himself pointed out that such models generally were not consistent with the occurence of the first power of the frequence in spectral formulae such as those of Balmer).

Formulation of Problem

The equation of motion of a uniform beam is

$$EI\frac{\partial^4 y}{\partial x^4} + m\frac{\partial^2 y}{\partial t^2} = 0 \tag{1}$$

where

E = modulus of elasticity
I = moment of inertia of beam cross section with respect to neutral axis
m = mass per unit length of beam
y = transverse displacement
x = coordinate measured along beam
t = time

Assuming a harmonic time dependence of angular frequency ω, we may replace $(\partial^2 y/\partial t^2)$ by $-\omega^2 y$. In the formulation of the boundary value problem for a beam supported at $x = 0, \ell, 2\ell, \text{- -} N\ell$ (Fig. 1) we also find it convenient to introduce a dimensionless, local coordinate such that

$$y = y_n(\xi), \quad n = 1, 2, \cdots N \tag{2a}$$

$$\xi = \frac{x}{\ell} - (n-1), \quad (n-1)\ell \leq x \leq n\ell \tag{2b}$$

Introducing, in addition, the dimensionless, eigenvalue parameter

$$\lambda^4 = m\omega^2\ell^4/EI \tag{3}$$

(1) goes over to

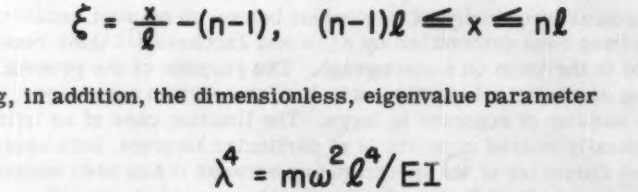

Fig. 1. A beam resting on uniformly spaced supports.

$$\frac{d^4 y_n}{d\xi^4} - \lambda^4 y_n = 0, \quad n = 1, 2, \cdots N \tag{4}$$

We shall assume that the beam is simply supported at the end points as well as the intermediate points, although the following method of solution is equally amenable to other end conditions (the modification of the intermediate support conditions,* on the other hand, would be rather more involved). The boundary conditions then read

$$y_n(0) = y_n(1) = 0, \quad n = 1, 2, \cdots N \tag{5a}$$

$$y'_{n-1}(1) = y'_n(0), \quad n = 2, 3, \cdots N \tag{5b}$$

$$y''_{n-1}(1) = y''_n(0), \quad n = 2, 3, \cdots N \tag{5c}$$

$$y''_1(0) = y''_N(1) = 0 \tag{5d}$$

Solution

The most general solution to (4) that satisfies (5a) is given by

$$y_n(\xi) = A_n[\sinh\lambda \sin\lambda\xi - \sin\lambda \sinh\lambda\xi] + B_n[\sinh\lambda \sin\lambda(1-\xi) - \sin\lambda \sinh\lambda(1-\xi)] \tag{6a}$$

In order to avoid indeterminate forms, we find it convenient to treat separately those modes that are identical with those of a single span of length ℓ - viz.,

$$y_n(\xi) = \sin\lambda\xi, \quad \sin\lambda = 0 \tag{6b}$$

which clearly satisfy all of (5a,b,c,d).

We first impose the moment continuity condition (5c) on (6a) to obtain

$$B_n = A_{n-1} \tag{7}$$

Substituting (7) in (6a) and imposing the slope continuity condition (5b) on the result then yields the difference equation

$$A_{n+1} - 2\cos\theta A_n + A_{n-1} = 0 \tag{8}$$

---

* E.g., to elastic supports. We remark that clamping the beam at the intermediate supports would render the motion of the successive bays independent.

where we have introduced the parameter θ according to

$$\cos\theta = (\sinh\lambda - \sin\lambda)^{-1}(\sinh\lambda\cos\lambda - \sin\lambda\cosh\lambda) \tag{9}$$

The most general solution to (8) is given by

$$A_n = A\sin(n\theta) + B\cos(n\theta) \tag{10}$$

where $\underline{A}$ and $\underline{B}$ are arbitrary constants. The boundary conditions to be satisfied by this solution follow from the imposition of (5d) on (6a) and (7) and read

$$A_0 = A_N = 0 \tag{11}$$

Setting $\underline{A}_0 = 0$ in (10) yields $\underline{B} = 0$, whence $\underline{A}_N = 0$ requires $\sin(\underline{N}\theta)$ to vanish. We are free to choose any value of θ that satisfies the latter condition, but in what follows we find it expedient to choose

$$\theta = \theta_r = \pi\left[1 + \left(\frac{r-1}{N}\right)\right] \tag{12a}$$

$$\lambda_r = \lambda(\theta_r) \tag{12b}$$

where $\underline{r}$ is any positive integer, and (12b) implies $\theta = \theta_r$ in (9).

The solution to the boundary value problem presented by (4) and (5) now may be placed in the form*

$$y_n(\xi) = \sin(n\theta_r)\, f_r(\xi) + \sin(n-1)\theta_r\, f_r(1-\xi) \tag{13}$$

$$f_r(\xi) = \sinh\lambda_r\, \sin\lambda_r\xi - \sin\lambda_r\, \sinh\lambda_r\xi \tag{14}$$

This form of the solution is indeterminate if λ is an integral multiple of π, but then we may resort directly to (6b).

The Frequency Spectra

We now proceed to examine those values of λ determined by (9) and (12), which, in turn, determine the permissible frequencies of free vibration *via* (3). We first remark that π is the smallest value of λ for which θ, as given by (9), is real -- *viz.*, $\cos\theta = -1$, corresponding to which we choose $\theta = \pi$ and $\underline{r} = 1$. Setting $\underline{r} = 1,2,3,$—N then yields the successive values

$$\pi = \lambda_1 < \lambda_2 < \cdots < \lambda_N < 1.5056\pi \tag{15a}$$

---
* Illustrative plots of these mode shapes are given in footnote ref. 1.

Setting r = N + 1 gives a value of λ between λ_N and 1.5056π, but the corresponding solution given by (13) vanishes identically and is discarded as trivial. There are, however, no values of λ in the interval $(1.5056\pi, 2\pi)$ that yield real θ, and we find as the next sequence

$$2\pi = \lambda_{N+1} < \lambda_{N+2} < \cdots < \lambda_{2N} = 2.4998\pi \qquad (15b)$$

etc., the general sequence being given approximately by*

$$s\pi = \lambda_{(s-1)N+1} < \cdots < \lambda_{Ns} < (s+\tfrac{1}{2})\pi + 2(-)^{s+1}\, e^{-(s+\frac{1}{2})\pi} + O\left[e^{-(2s+1)\pi}\right], \quad s = 1, 2, \cdots \qquad (15c)$$

These conclusions are illustrated graphically in Fig. 2, the numerical values shown there corresponding to N = 6.

The large values of the hyperbolic functions for $\lambda > \pi$ naturally suggest the use of the asymptotic approximation (differing from the exact result (9) by at most 0.02)

$$\cos\theta \doteq \cos\lambda - \sin\lambda, \qquad \lambda \geq \pi \qquad (16a)$$

or, equivalently,

$$\sin 2\lambda \doteq \sin^2\theta, \quad \lambda \geq \pi \qquad (16b)$$

In this approximation we have only to determine the first sequence λ_1, λ_2, $--\lambda_N$ from (16b), after which the remaining λ_r satisfy the (approximate) periodicity condition

$$\lambda_{r+(s-1)N} = \lambda_r + (s-1)\pi, \quad r = 1, 2, \cdots N, \quad s = 1, 2, \cdots \qquad (17)$$

Semi-infinite and Infinite Arrays

The results of the preceding section remain valid as N tends to infinity (semi-infinite array), but then θ may assume any value, and λ may assume all values for which the magnitude of the right hand side of (9) is smaller than unity. The sequences of (15) then go over to blocks of continuous spectra - viz.,

---

* The right hand, upper bounds in (15c) follow from setting $\theta = (s+1)\pi$ in (9) and correspond to the natural frequencies of a single span beam with clamped ends.

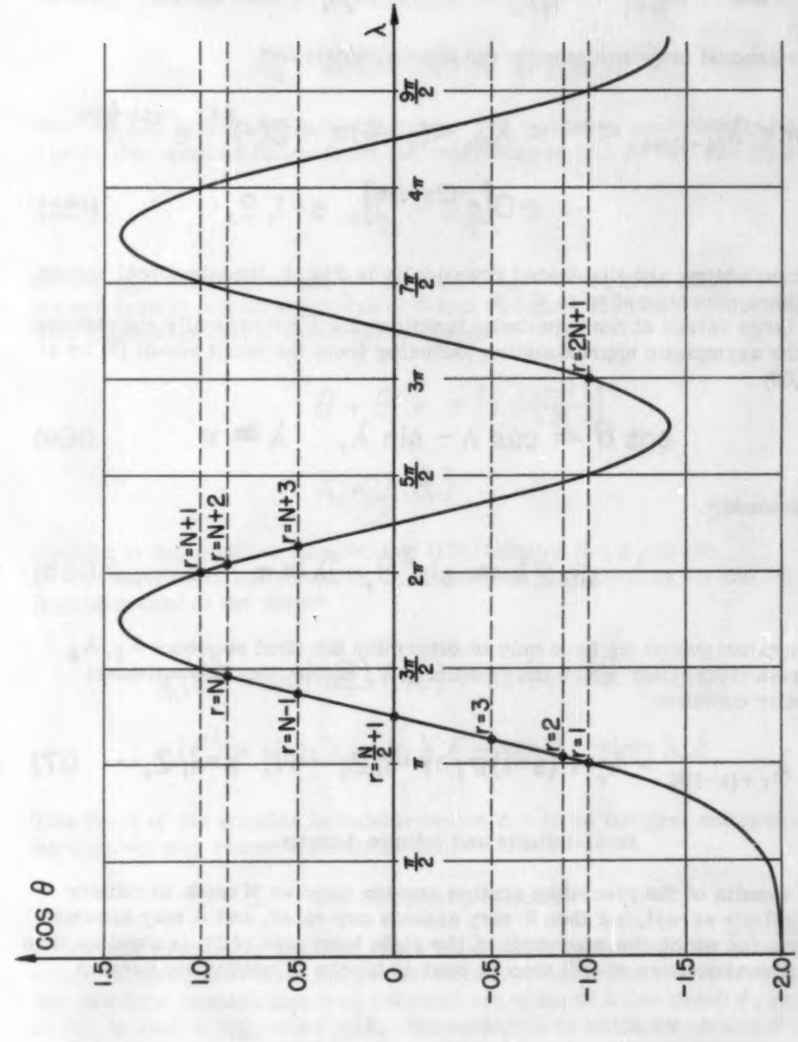

Fig. 2. Illustrating the permissible values of λ and θ. The undulating curve is given by the right hand side of Eq. (9) and the permissible values of θ by Eq. (12). The numerical values shown correspond to the particular case N = 6.

$$s\pi \leq \lambda(\theta) \leq (s+\tfrac{1}{2})\pi + 2(-)^{s+1} e^{-(s+\frac{1}{2})\pi}$$
$$+ O\left[e^{-(2s+1)\pi}\right], \quad s\pi \leq \theta \leq (s+1)\pi \qquad (18)$$

We remark that the character of the spectra represented by (18) might have been anticipated by analogy with the properties of band pass filters. In contrast to the spectrum of a filter made up of discrete elements, however, the number of pass bands for the continuous beam is infinite, although there can be no free oscillation below the minimum cutoff frequency corresponding to $\lambda = \pi$.

If we assume the array to be <u>fully infinite</u> (periodically supported, with $n = -\infty, ---, -1, 0, 1, ---\infty$) the spectra are still given by (18), but we no longer are required to reject the solution $\cos(n\theta)$ to the difference equation (8) and must add to (13) a second, independent solution in which $\cos(n\theta)$ replaces $\sin(n\theta)$. Alternatively, we may write

$$y_n = e^{in\theta} f_\lambda(\xi) + e^{i(n-1)\theta} f_\lambda(1-\xi) \qquad (19)$$

where $f_\lambda(\xi)$ is given by (14) with λ depending on θ through (9).

Restoring the time factor $e^{i\omega t}$, the solution (19) represents a disturbance travelling in the negative or positive x direction as θ is positive or negative, respectively. The wavelength of this disturbance is given by [6] $2\pi\ell/\theta$ and is integrally related to ℓ only when θ is an integral multiple of π. It follows that the <u>phase</u> velocity is given by[7]

$$V = \omega\ell/\theta \qquad (20)$$

where, we recall, θ depends on ω through (3) and (9). The <u>group</u> velocity then is given by[8]

$$U = \ell \frac{d\omega}{d\theta} \qquad (21)$$

The derivative $(d\omega/d\theta)$ may be evaluated from (3) and (9); it is, of course, real only when θ is real but then has the same sign as θ — <u>i.e.</u>, the phase and group velocities are of the same sign (that U and V could be of opposite sign is not inconceivable). The corresponding values of U and V for an infinite, unsupported beam are given by [let $y = e^{i\omega(t-x/v)}$ in (1)]

$$V_\infty = \tfrac{1}{2}U_\infty = \left(\frac{EI}{m}\right)^{\frac{1}{4}} \omega^{\frac{1}{2}} = \ell^{-1}\left(\frac{EI}{m}\right)^{\frac{1}{2}} \lambda \qquad (22)$$

whence

$$V/V_\infty = \lambda/\theta \qquad (23)$$

$$U/U_\infty = d\lambda/d\theta \tag{24}$$

On the basis of the approximation (16) these ratios become

$$V/V_\infty \simeq \lambda/\sin^{-1}(\sin 2\lambda)^{\frac{1}{2}} \tag{25}$$

$$U/U_\infty \simeq (\sin 2\lambda)^{\frac{1}{2}}/(\cos\lambda + \sin\lambda) \tag{26}$$

The approximations (25) and (26) are plotted in Fig. 3. We observe that the phase velocity ratio decreases monotonically from 1 to $1 - (2s + 2)^{-1}$ as λ increases from $s\pi$ to $(s + 1/2)\pi$, whereas the group velocity ratio vanishes at both ends of these intervals and achieves the maximum value $2^{-1/2}$ at the midpoints of the intervals. These properties are again generalizations of their counterparts for a discrete element, band pass filter; in particular, the vanishing of the group velocity is associated with the existence of standing waves corresponding to the independent vibrations of the individual spans at frequencies corresponding to pinned or clamped ends as $\lambda = s\pi$ or $(\underline{s} + 1/2)\pi$, respectively.

We conclude by noting that properties similar to those discussed in the present paper are characteristic of any continuous system subjected to intermediate constraints, a fact first noted by Kelvin (1881).[9] Numerous examples are given by Brillouin,[10] but the problems associated with beams are unique insofar as they are governed by a differential equation of fourth order.

February 19, 1955

REFERENCES

1. R. S. Ayre and L. S. Jacobsen, Natural Frequencies of Continuous Beams of Uniform Span Length, Jour. Appl. Mech. 17, 391-395 (1950); ibid. 18, 217 (1951).
2. J. M. Hedgepeth, B. Budiansky and R. W. Leonard, Analysis of Flutter in Compressible Flow of a Panel on Many Supports, Jour. Aeronaut. Sci. 21, 475 (1954).
3. L. Brillouin, Wave Propagation in Periodic Structures (Dover Publ., New York, 1953), p. 2; Brillouin gives an extensive historical survey and many examples.
4. Lord Rayleigh, On the Propagation of Waves along Connected Systems of Similar Bodies, Philosoph. Mag. 44, 356 (1897); Sci. Papers 4, 340.
5. __________, On Iso-Periodic Systems, Philosoph. Mag. 46, 567 (1898); Sci. Papers 4, 367.
6. Rayleigh, footnote ref. 4.
7. ibid.
8. Rayleigh, Theory of Sound, vol. 1 (Dover Publ., New York, 1945), p. 475.
9. Brillouin, footnote ref. 3, p. 11.
10. op. cit.

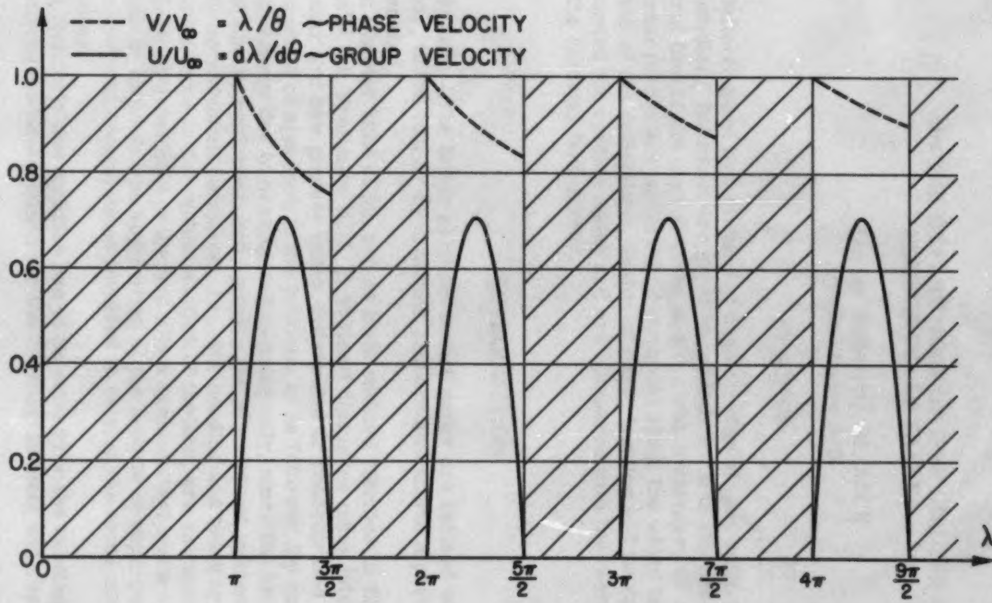

Fig. 3. The phase and group velocities for a periodically supported beam expressed as fractions of the corresponding velocities for an infinite, unsupported beam. See Eqs. (25) and (26).

Paper 870 EM 1

JOURNAL

ENGINEERING MECHANICS DIVISION

Proceedings of the American Society of Civil Engineers

ON THE DEFLECTIONS OF BOW GIRDERS OF NON-CIRCULAR SHAPES

Enrico Volterra,[1] M. ASCE
(Proc. Paper 870)

SYNOPSIS

Deflections of bow girders of non-circular shapes built-in at both ends are studied. Solutions are given in explicit form in the cases in which the central line of the curved beam is a cycloid, a catenary or a parabola and the external forces are uniformly distributed along the whole length of the beam. Curves of the deflections, angles of twist, bending and twisting moments are presented for certain cases and are compared with the corresponding values for the circular bow-girder.

INTRODUCTION

Notation—The letter symbols in this paper are defined where they first appear, in the text or by diagram, and are assembled alphabetically in Appendix I.

In Chapter Nine of his recent book entitled "Studies in Elastic Structures"[2] (1), Professor A. J. S. Pippard discusses many interesting cases of circular arc bow girders under distributed or concentrated external loads. His method of approach to the problem is as follows: By expressing the total strain energy due to bending and twisting only, since the contribution due to shear can be neglected, and applying the principle of minimum strain energy, the three redundant unknowns, i.e., the bending and twisting moments and shearing force in the middle section of the arc, are calculated.

If the external load is divided into a symmetrical and a skew-symmetrical system of loadings, the application of the method of superposition simplifies the numerical computations involved in solving the three simultaneous equations.

In fact, only one equation has to be solved for the bending moment, and two simultaneous equations for the twisting moment and shearing force.

Note: Discussion open until May 1, 1956. Paper 870 is part of the copyrighted Journal of the Engineering Mechanics Division of the American Society of Civil Engineers, Vol. 82 No. EM 1, January, 1956.

1. Professor of Mechanics, Rensselaer Polytechnic Institute, Troy, New York.
2. Numbers in parentheses refer to the Bibliography at the end of the paper.

Summing up algebraically the results of the two cases dealt with separately, the final required solutions are obtained.

But in the more general cases of non-circular arc bow girders fixed at both ends Professor Pippard finds that the resulting expressions "cannot usually be integrated by exact mathematical process but must be calculated approximately by graphical or arithmetical methods."

However, it can be shown that also in the case of a non-circular bow girder built-in at both ends and subjected to a uniformly distributed load the results can be expressed in closed form if the central line of the curved beam is a cycloid, a catenary or a parabola.

In order to obtain these results, a different and more general method of approach than the one described by Professor Pippard in his book, has to be applied. In fact, four differential equations connecting the bending moment M_x, the twisting moment M_z, the deflection v, the twisting angle β, the initial curvature R of the central line of the beam, and its inertia characteristics EI_x and torsional characteristics K have to be used.

Two of these equations are the well-known De-Saint Venant's equations for a curved beam bent out of its plane of initial curvature(2,3), while the two subsidiary equations of equilibrium are obtained by expressing the conditions of equilibrium of the beam.

The method just described is the same as the one already used in previous papers in the study of problems of deflections of circular rings on rigid supports and circular arc bow girders under distributed or concentrated forces(4), and of circular rings supported by elastic foundations and subjected to concentrated symmetric or antisymmetric forces(5,6,7).

But, due to the fact that in the present case the curvature R of the central line of the bar is not constant, the solution of the system of differential equations is more laborious than in problems of circular beams. However, since in the particular cases in which the central line of the beam is a cycloid, a catenary or a parabola the relationships between radius of curvature R in a generic point of the central line whose normal makes the angle ψ with the axis of symmetry of the beam (see Fig. 1) and the curvature R_o at the central point P_o are expressed by the following simple formulas:

for the cycloid: $$R = R_o \cos\varphi$$

for the catenary: $$R = \frac{R_o}{\cos^2\varphi}$$

for the parabola: $$R = \frac{R_o}{\cos^3\varphi}$$

and if the external forces are uniformly distributed along the whole length of the beam, then the results for the bending and twisting moments, deflections and angles of twist can be expressed in closed form.

Graphs of the deflections, angles of twist, bending and twisting moments are presented for certain cases and are compared with the corresponding values for the bow girder of circular shape.

In the preparation of these graphs the author acknowledges with thanks the help given by Messers T. E. Edelbaum and E. C. Zachmanoglou, both

students in the Department of Aeronautical Engineering at Rensselaer Polytechnic Institute, and the help by the "Istituto per le Applicazioni del Calcolo" of the Italian "Consiglio Nazionale delle Ricerche," Rome, Italy, in connection with some of the numerical computation involved.

The Equations of the Problem

The beam will be referred to a system of rectangular coordinates OXYZ with the origin O at the centroid of the cross-section, the axes X and Y coinciding with the principal axes of inertia of the cross-section, and the axis Z with the tangent to the center line at O, as shown in Fig. 2a. If M_X and M_Z are the moments acting on the cross-section at O about the X and Z axes respectively (bending and twisting moments on the generic section of the beam), v the displacement of the centroid O in the direction of the Y axis, β the angle of twist of the cross-section about the Z axis, EI_X the flexural rigidity, K the torsional rigidity, R the initial radius of curvature of the center line of the bar, the following two equations will be verified[2,3]:

$$\left.\begin{aligned} EI_x\left[\frac{\beta}{R} - \frac{d^2v}{dS^2}\right] &= M_x \\ k\theta = k\left[\frac{d\beta}{dS} + \frac{1}{R}\frac{dv}{dS}\right] &= M_z \end{aligned}\right\} \qquad (1)$$

The equations of equilibrium are:

$$\left.\begin{aligned} \frac{d}{dS}\left[\frac{dM_x}{dS} + \frac{M_z}{R}\right] &= p \\ \frac{dM_z}{dS} - \frac{M_x}{R} &= 0 \end{aligned}\right\} \qquad (2)$$

where p represents the external load, which is supposed uniformly distributed along the whole length of the bar.*

*Equations (2) can be obtained by expressing the conditions of equilibrium of an element of the bar of length dS. In fact the following equations can easily be derived from Figure 2b:

$$2M_x \sin\frac{d\alpha}{2} + M_z - (M_z + dM_z) = 0$$

but, since:

$$2\sin\frac{d\alpha}{2} = d\alpha = \frac{dS}{R}$$

$$M_x d\alpha - dM_z = 0$$

In the case in which the arc of length 2ℓ is symmetrical with respect to point P_o (see Figure 1) the conditions of fixity of both extremities of the beam imply the following boundary conditions:

$$\beta(\pm\ell) = v(\pm\ell) = \frac{dv(\pm\ell)}{dS} = 0 \qquad (3)$$

Introducing as new variables the adimensional quantities:

$$m_x = \frac{M_x}{pR_o^2}$$

$$m = \frac{M_z}{pR_o^2}$$

$$x = \frac{\beta}{\lambda} \qquad (4)$$

$$y = \frac{1}{\lambda}\frac{dv}{dS}$$

where:

$$\lambda = \frac{1}{2}\, pR_o^3 \left(\frac{1}{k} + \frac{1}{EI_x} \right)$$

---

*Continued from page 3.

from which the equation $\frac{M_x}{R} - \frac{dM_z}{dS} = 0$ follows.

$$V - (V+dV) + pdS = 0 \quad \text{or} \quad \frac{dV}{dS} = p$$

$$M_x - (M_x+dM_x) + VdS - M_z \sin d\alpha = 0$$

or $$- dM_x + VdS - M_z\, d\alpha = 0$$

$$V = \frac{dM_x}{dS} + M_z\frac{d\alpha}{dS} = \frac{dM_x}{dS} + \frac{M_z}{R}$$

$$p = \frac{dV}{dS} = \frac{d}{dS}\left[\frac{dM_x}{dS} + \frac{M_z}{R}\right]$$

and assuming as independent variable the angle ψ that the normal to the central line of the beam in a generic point P makes with the axis of symmetry at P_o (see Figure 1), equations (1) and (2) become:

$$\frac{dx}{d\varphi} + y - \rho(\mu+1)m_z = 0$$

$$\frac{dy}{d\varphi} - x - \rho(\mu-1)m_x = 0$$

$$\frac{dm_x}{d\varphi} + m_z = \Psi + C\rho \qquad (5)$$

$$\frac{dm_z}{d\varphi} - m_x = 0$$

where:

$$\mu = \frac{\frac{1}{C} - \frac{1}{EI_x}}{\frac{1}{C} + \frac{1}{EI_x}} \quad , \qquad \Psi = \rho\sigma$$

$$\rho = \frac{R}{R_o} \quad , \qquad \sigma = \int_o^{\varphi} \rho \, d\varphi$$

$$y = \frac{du}{d\sigma} = \frac{1}{\lambda}\frac{dv}{dS} \quad , \qquad u = \frac{v}{\lambda R_o}$$

---

*Continued from page 4.
Equations (2) could also be obtained by minimizing the potential energy of the bar, which, considering only the terms due to bending and twisting moments, since, as pointed out by Professor Pippard the term due to shear can be neglected, will be expressed by:

$$U = \frac{1}{2}\int_{S_1}^{S_2} \left[\frac{M_x^2}{EI_x} + \frac{M_z^2}{k}\right] dS - p\int_{S_1}^{S_2} v dS$$

and C is a constant of integration to be determined from the boundary equations (3) or:

$$\beta(\pm\alpha) = v(\pm\alpha) = y(\pm\alpha) = 0 \qquad (6)$$

Case of the Circle

In this particular case:

$$\rho = 1$$

$$\sigma = \varphi$$

and the solution of equations (5) and (6) gives:

$$m_x = 1 + A\cos\varphi$$

$$m_z = \quad + A\sin\varphi$$

$$X = \left[2 + A\varphi\sin\varphi - \cos\varphi\left(\frac{2}{\cos\varphi} + A\alpha\tan\alpha\right)\right]$$

$$U = \frac{1}{(1+\mu')}\left[\varphi^2 - \alpha^2 - 2(\mu'+1)\left(1 - \frac{\cos\varphi}{\cos\alpha}\right)\right] +$$

$$+ \frac{1}{(1+\mu')} A\left\{-(\mu'+1)\varphi\sin\varphi + \left[(\mu'+1)\alpha\tan\alpha - 2\right]\cos\varphi + 2\cos\alpha\right\}$$

where:

$$\mu' = \frac{1-\mu}{1+\mu}$$

$$A = 2\frac{\alpha\cos\alpha - (1+\mu')\sin\alpha}{(1+\mu')\alpha + (\mu'-1)\sin\alpha\cos\alpha}$$

in accordance with the results already obtained in a previous paper(4) but using a different notation.

Case of the Cycloid

In this particular case:

$$\rho = \cos\varphi$$

$$\sigma = \sin\varphi$$

and the solution of equations (5) and (6) gives:

$$m_x = -\frac{1}{3}\cos 2\varphi + \frac{1}{4}A\cos\varphi$$

$$m_z = -\frac{1}{6}\sin 2\varphi + \frac{1}{4} A \sin\varphi$$

$$x = \frac{1}{24}\left\{\frac{5+\mu}{4}\cos 3\varphi - (3+\mu) A \cos 2\varphi + B\cos\varphi - (3-\mu)\varphi\sin\varphi + \right.$$

$$\left. + 3(1-\mu) A\right\}$$

$$u = \frac{1}{96}\left\{-\frac{7-5\mu}{8}\cos 4\varphi + \frac{2}{3} A(3-\mu)(\cos 3\varphi + 3\cos\varphi) - \right.$$

$$\left. - \left[B + \frac{5}{4}(1-3\mu)\right]\cos 2\varphi + (3-\mu)\varphi(\varphi + \sin 2\varphi) + C\right\}$$

where:

$$A = \frac{\frac{1-3\mu}{4}\sin 4\alpha + 2(1-\mu)\sin 2\alpha + (3-\mu)\alpha}{3(2-\mu)\sin\alpha - \mu\sin 3\alpha}$$

$$B = \mu A(\cos 3\alpha + 3\cos\alpha) - \frac{1-3\mu}{4}(3-\cos 4\alpha) - (1+\mu)\cos 2\alpha$$

$$C = \frac{7-5\mu}{8}\cos 4\alpha - \frac{2}{3} A(3-\mu)(\cos 3\alpha + 3\cos\alpha) +$$

$$+ \left[B + \frac{5}{4}(1-3\mu)\right]\cos 2\alpha - (3-\mu)\alpha(\alpha + \sin 2\alpha)$$

Case of the Catenary

In this particular case:

$$\rho = \frac{1}{\cos^2\varphi}$$

$$\sigma = \tan\varphi$$

and the solution of equations (5) and (6) gives:

$$m_x = A\cos\varphi + \frac{1}{2\cos^2\varphi} + \frac{1}{2} - \frac{1}{4}\sin\varphi \log\frac{1+\sin\varphi}{1-\sin\varphi}$$

$$m_z = A\sin\varphi + \frac{1}{2}\tan\varphi + \frac{1}{4}\cos\varphi\log\frac{1+\sin\varphi}{1-\sin\varphi}$$

$$x = \frac{(1+\mu)A}{\cos\varphi} - 2\mu A(\varphi\sin\varphi + \cos\varphi\log|\cos\varphi|) + B\cos\varphi + \frac{2+\mu}{6\cos^2\varphi} -$$

$$- \frac{2-3\mu}{2} + \frac{2-3\mu}{4}\sin\varphi\log\frac{1+\sin\varphi}{1-\sin\varphi} + \mu\left[F_1(\varphi)\cos\varphi + F_2(\varphi)\sin\varphi\right]$$

$$u = -2\mu A[\frac{1}{\cos\varphi} + \frac{\log|\cos\varphi|}{\cos\varphi} - \frac{1}{2}\varphi\log\frac{1+\sin\varphi}{1-\sin\varphi} + F_1(\varphi) + \frac{B}{\cos\varphi} -$$

$$- \frac{1-\mu}{24\cos^4\varphi} - \frac{5-7\mu}{8\cos^2\varphi} - \frac{3-\mu}{32}\log^2\frac{1+\sin\varphi}{1-\sin\varphi} + \frac{1-\mu}{8}\frac{\sin\varphi}{\cos^2\varphi}\log\frac{1+\sin\varphi}{1-\sin\varphi} +$$

$$+ \mu\left[\frac{1}{\cos}F_1(\varphi) - \frac{1}{2}F_2(\varphi)\log\frac{1+\sin\varphi}{1-\sin\varphi} + F_3(\varphi)\right] + C$$

where:

$$A = \frac{\frac{1}{2}\frac{\sin\alpha}{\cos^2\alpha} + \frac{1-2\mu}{4}\log\frac{1+\sin\alpha}{1-\sin\alpha} + \mu F_2(\alpha)}{2\mu\alpha - (1+\mu)\tan\alpha}$$

$$B = -A\left[1 + \mu - 2\mu\log|\cos\alpha|\right] + \frac{1-\mu}{6\cos^3\alpha} + \frac{1-3\mu}{2\cos\alpha} -$$

$$- \frac{1-\mu}{4}\tan\alpha\log\frac{1+\sin\alpha}{1-\sin\alpha} - \mu F_1(\alpha)$$

$$C = 2\mu A\left[\frac{1}{\cos\alpha} + \frac{\log|\cos\alpha|}{\cos\alpha} - \frac{1}{2}\alpha\log\frac{1+\sin\alpha}{1-\sin\alpha} + F_1(\alpha)\right] - \frac{B}{\cos\alpha} +$$

$$+ \frac{1-\mu}{24\cos^4\alpha} + \frac{5-7\mu}{8\cos^2\alpha} + \frac{3-\mu}{32}\log^2\frac{1+\sin\alpha}{1-\sin\alpha} - \frac{1-\mu}{8}\frac{\sin\alpha}{\cos^2\alpha}\log\frac{1+\sin\alpha}{1-\sin\alpha} -$$

$$- \mu\left[\frac{1}{\cos\alpha}F_1(\alpha) - \frac{1}{2}F_2(\alpha)\log\frac{1+\sin\alpha}{1-\sin\alpha} + F_3(\alpha)\right]$$

$$F_1(\varphi) = \frac{1}{2}\int_0^{\varphi}\log\frac{1+\sin p}{1-\sin p}\,dp$$

$$F_2(\varphi) = \frac{1}{2}\int_0^{\varphi} \tan p \log \frac{1+\sin p}{1-\sin p}\, dp \tag{7}$$

$$F_3(\varphi) = \frac{1}{4}\int_0^{\varphi} \tan p \log^2 \frac{1+\sin p}{1-\sin p}\, dp$$

Case of the Parabola

In this particular case:

$$\rho = \frac{1}{\cos^3\varphi}$$

$$\sigma = \frac{1}{2}\left[\frac{\sin\varphi}{\cos^2\varphi} + \frac{1}{2}\log\frac{1+\sin\varphi}{1-\sin\varphi}\right]$$

and the solution of equations (5) and (6) gives:

$$m_x = A\cos\varphi + \frac{1}{2}\left[\frac{1}{\cos^2\varphi} + \frac{5}{4}\right]\sigma\sin\varphi - \frac{1}{8\cos^4\varphi} - \frac{5}{24\cos^2\varphi}$$

$$m_z = A\sin\varphi + \frac{1}{2}\left[\frac{1}{\cos^2\varphi} - \frac{5}{4}\right]\sigma\cos\varphi - \frac{5\sin\varphi}{24\cos^2\varphi}$$

$$x = (1-3\mu)A\sigma\sin\varphi + \frac{2A\mu}{\cos^2\varphi} + B\cos\varphi - \frac{3\mu}{4}\sigma^2\cos\varphi +$$

$$+\frac{5+3\mu}{24}\sigma\frac{\sin\varphi}{\cos^3\varphi} - \frac{11+7\mu}{120\cos^5\varphi} - \frac{2(1-3\mu)}{45}\left(\frac{1}{\cos^3\varphi} + \frac{4}{\cos\varphi}\right)$$

$$u = (1-3\mu)A\left[\frac{1}{3\cos^3\varphi} - \sigma\tan\varphi\right] + \frac{B}{2\cos^2\varphi} - \frac{3\mu}{8}\frac{\sigma^2}{\cos^2\varphi} -$$

$$-\frac{5(3-19\mu)}{128}\sigma^2 - \frac{(1-\mu)}{48}\sigma\frac{\sin\varphi}{\cos^6\varphi} - \frac{5(3-19\mu)}{192}\sigma\frac{\sin\varphi}{\cos^4\varphi} +$$

$$+\frac{(1-\mu)}{128\cos^8\varphi} + \frac{203-859\mu}{5760\cos^6\varphi} + \frac{2(1-3\mu)}{45\cos^4\varphi} + C$$

where:

$$A = \frac{-\left(\dfrac{1}{3\cos^2\alpha} - \dfrac{5}{4}\mu\right)\dfrac{\sigma(\alpha)}{\cos\alpha} + \dfrac{(8+\mu)}{60}\dfrac{\sin\alpha}{\cos^5\alpha} + \dfrac{8(1-3\mu)}{45}\tan\alpha\left[\dfrac{1}{\cos^2\alpha} + 2\right]}{(1-3\mu)\sigma(\alpha) + 2\mu\dfrac{\sin\alpha}{\cos^2\alpha}}$$

$$B = -\frac{2\mu}{\cos\alpha}A + \frac{3\mu}{4}\left[\sigma(\alpha)\right]^2 + \frac{\sin\alpha}{8\cos^2\alpha}\left[\frac{1-\mu}{\cos^2\alpha} - 10\mu\right]\sigma(\alpha) -$$

$$-\frac{1-\mu}{24\cos^6\alpha} + \frac{5\mu}{12\cos^4\alpha} + \frac{16(1-3\mu)}{45}$$

$$C = (1-3\mu)A\left[\sigma(\alpha)\tan\alpha - \frac{1}{3\cos^3\alpha}\right] - \frac{B}{2\cos^2\alpha} + \frac{3\mu}{8}\frac{\left[\sigma(\alpha)\right]^2}{\cos^2\alpha} +$$

$$+\frac{5(3-19\mu)}{128}\left[\sigma(\alpha)\right]^2 + \frac{1-\mu}{48}\sigma(\alpha)\frac{\sin\alpha}{\cos^6\alpha} + \frac{5(3-19\mu)}{192}\sigma(\alpha)\frac{\sin\alpha}{\cos^4\alpha} -$$

$$-\frac{1-\mu}{128\cos^8\alpha} + \frac{859\mu-203}{5760\cos^6\alpha} + \frac{2(3\mu-1)}{45\cos^4\alpha}$$

In figures 3 to 10 the quantities m_x, m_z, x and u are given for the following values of the parameters $\alpha = 30°, 60°$; $\mu = -1/7$, $\mu = 0$, $\mu = 1/3$. In figure 11 the quantities m_x, m_z, x and u are given in the case of the cycloid and the circle for $\alpha = 90°$; $\mu = -1/7$, $\mu = 0$, $\mu = 1/3$. In figure 12 the functions $S(\psi)$ are given for the parabola, catenary and cycloid, while in figure 13 the values of the functions $F_1(\psi)$, $F_2(\psi)$ and $F_3(\psi)$ are given.

APPENDIX I. NOTATION

The following symbols, adopted for use in the paper, and for the guidance of discussers, conform essentially with American Standard Letter Symbols for Structural Analysis (ASA-Z10. 8-1942), prepared by a Committee of the American Standards Association, with Society representation and approved by the Association in 1942.

A	= a constant
B	= a constant
C	= a constant
E	= the modulus of elasticity
F_1, F_2, F_3	= functions defined by equation (7)

I_x = the rectangular moment of inertia
k = the torsional rigidity
M_x = bending moment
m_x $= \dfrac{M_x}{pR_o^2}$
M_z = twisting moment
m_z $= \dfrac{M_z}{pR_o^2}$
P_o = point of symmetry of the bar (defined in Fig. 1)
p = intensity of distributed load
R = the initial curvature of the center line of the beam
R_o = the initial curvature of the center line of the beam at point P_o
s = arc length
u $= \dfrac{v}{\lambda R_o}$
v = displacement along y axis
x, y, z = rectangular coordinate axes
α = an angle defined by equation (6) and by Fig. 1
β = the angle of twist
θ = the angle of twist per unit length
λ $= \dfrac{1}{2} pR_o^3 \left[\dfrac{1}{k} + \dfrac{1}{EI_x}\right]$
μ $= \dfrac{\dfrac{1}{k} - \dfrac{1}{EI_x}}{\dfrac{1}{k} + \dfrac{1}{EI_x}}$
σ $= \dfrac{S}{R_o}$
ρ $= \dfrac{R}{R_o}$
$d\psi$ $= \dfrac{dS}{R} = \dfrac{d}{\rho}$

APPENDIX II. BIBLIOGRAPHY

1. "Studies in Elastic Structures" by A. J. S. Pippard, Chapter 9, Bow Girders and Transversely Loaded Frames, Arnold and Co., London, 1952.

2. "Memoire sur le calcul de la résistance et de la flexion des pièces solides à simple ou à double courbure, en prenant simultanément en consideration les divers efforts auxquels elles peuvent être soumises dans tous les sens," by Barré De-Saint Venant, Comptes Rendus de L'Académie des Sciences de Paris, France, vol. 17, 1843, pp. 942-954 and 1020-1031.

3. "Strength of Materials—Advanced Theory and Problems," Part II, by S. Timoshenko, Macmillan and Co., New York, N. Y., 1936, pp. 467-473.

4. "Deflections of a Circular Beam Out of its Initial Plane" by E. Volterra, Paper No. 2727 Transactions of the American Society of Civil Engineers, vol. 120, 1955, p. 65-91.

5. "Bending of a Circular Beam Resting on an Elastic Foundation" by E. Volterra, Journal of Applied Mechanics, Trans. A.S.M.E., vol. 74, March 1952, pp. 1-4.

6. "Deflections of Circular Beams Resting on Elastic Foundations Obtained by Methods of Harmonic Analysis" by E. Volterra, Journal of Applied Mechanics, Trans. A.S.M.E., vol. 75, June 1953, pp. 227-232.

7. "Bending of a Constrained Circular Beam Resting on an Elastic Foundation" by E. Volterra and R. Chung, Proceedings of the American Society of Civil Engineers, vol. 79, Separate No. 205.

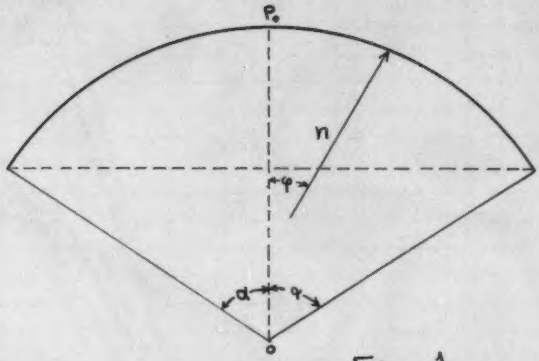

Fig. 1

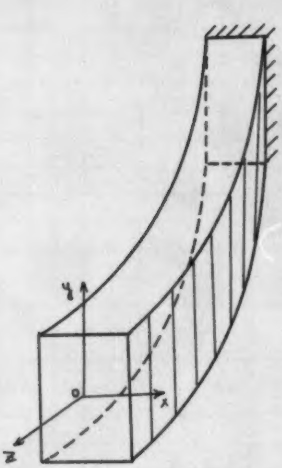

Fig. 2a

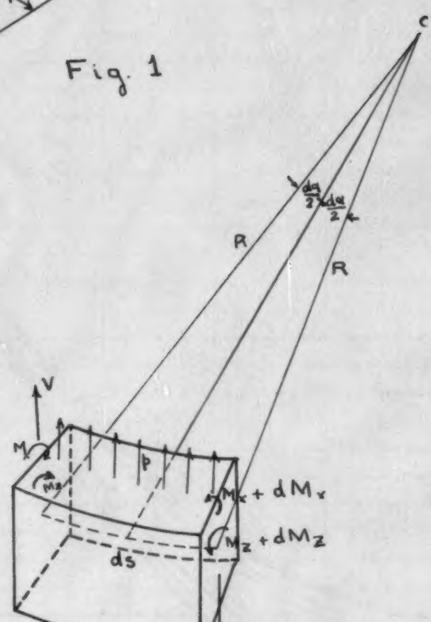

Fig 2b

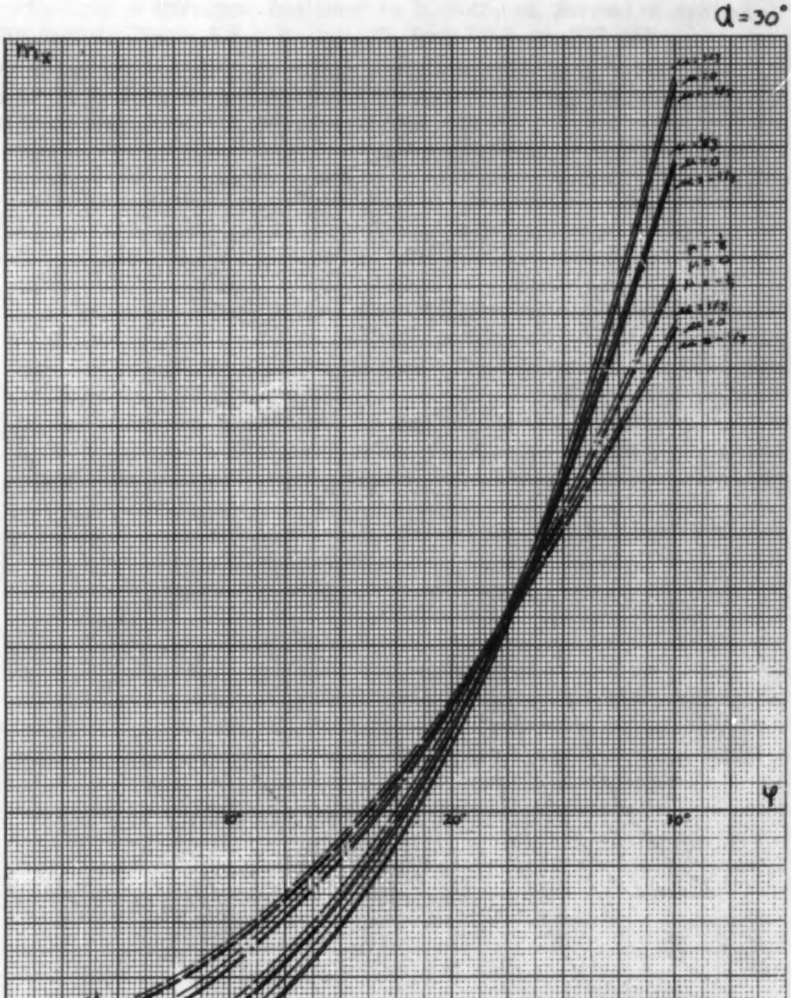

α = 30°
m_x
0.10
0.05
-0.05
φ
10°
20°
30°
cycloid
circle
catenary
parabola

Fig. 3

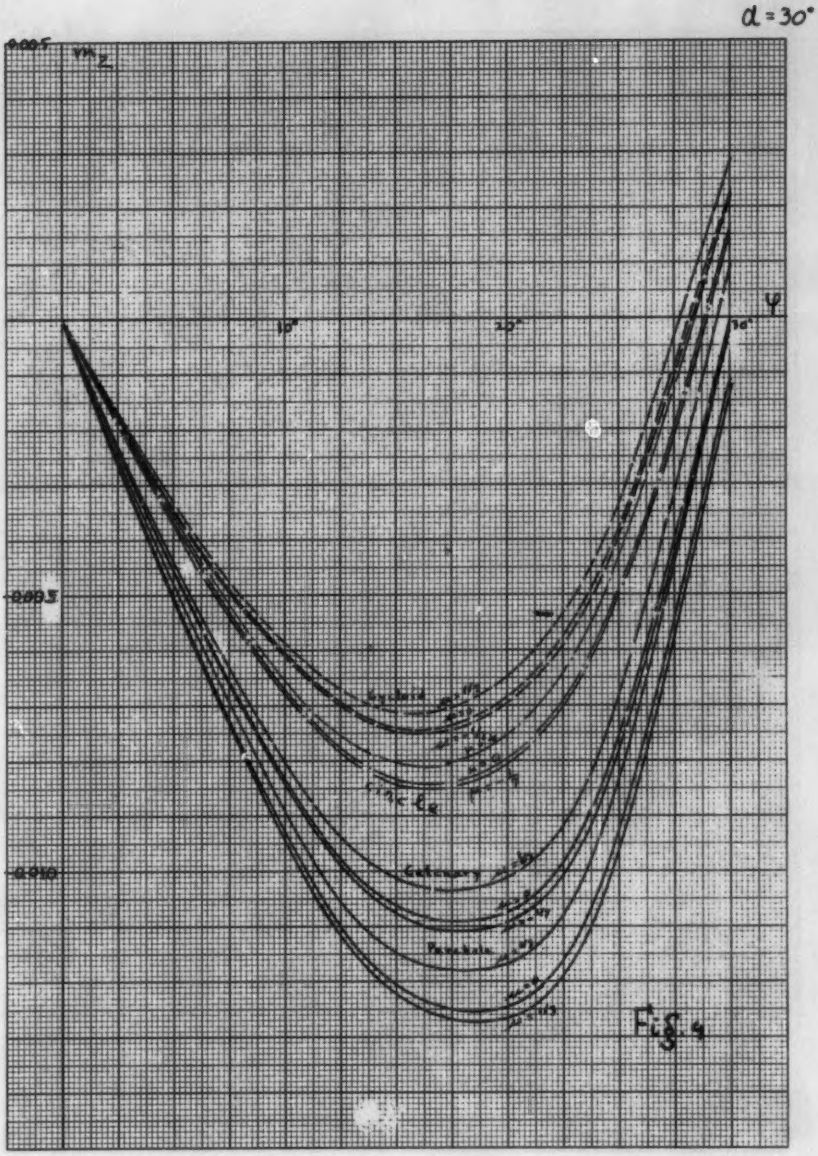
α = 30°
0.005
m_z
ψ
10°
20°
30°
0.005
0.010
Cycloid
Catenary
Parabola
Fig. 4

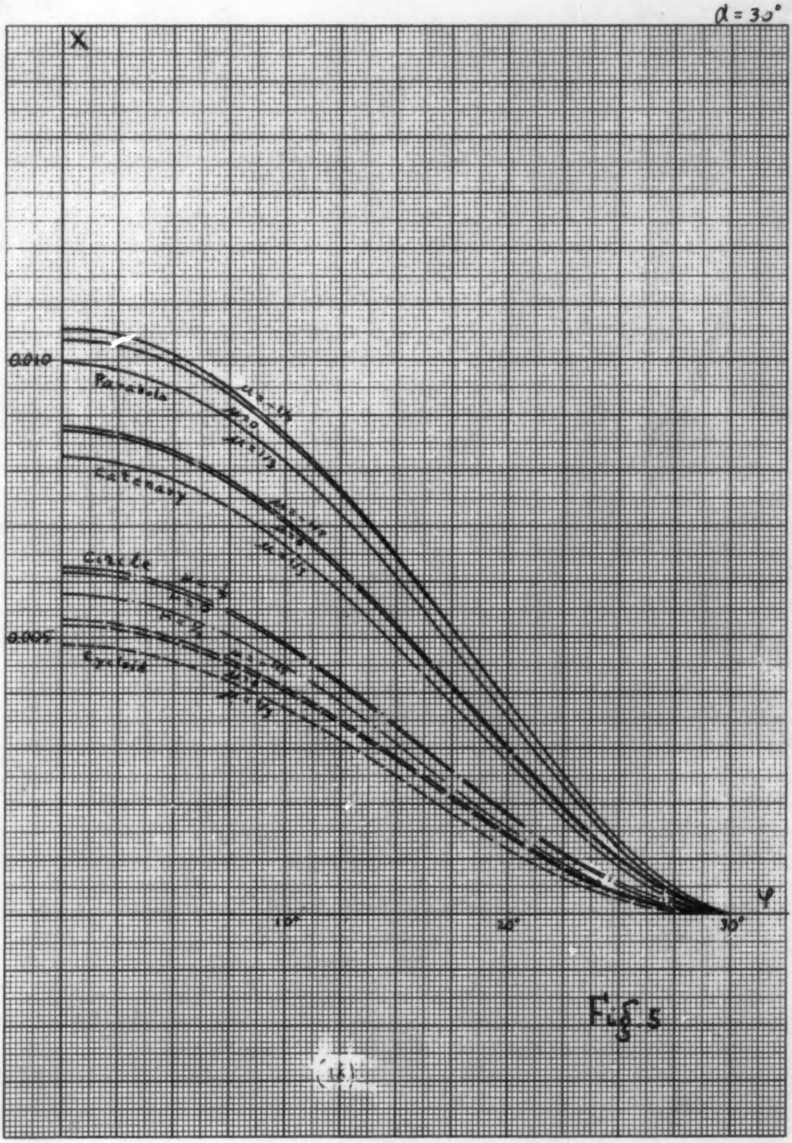

Fig. 5

$\alpha = 30°$

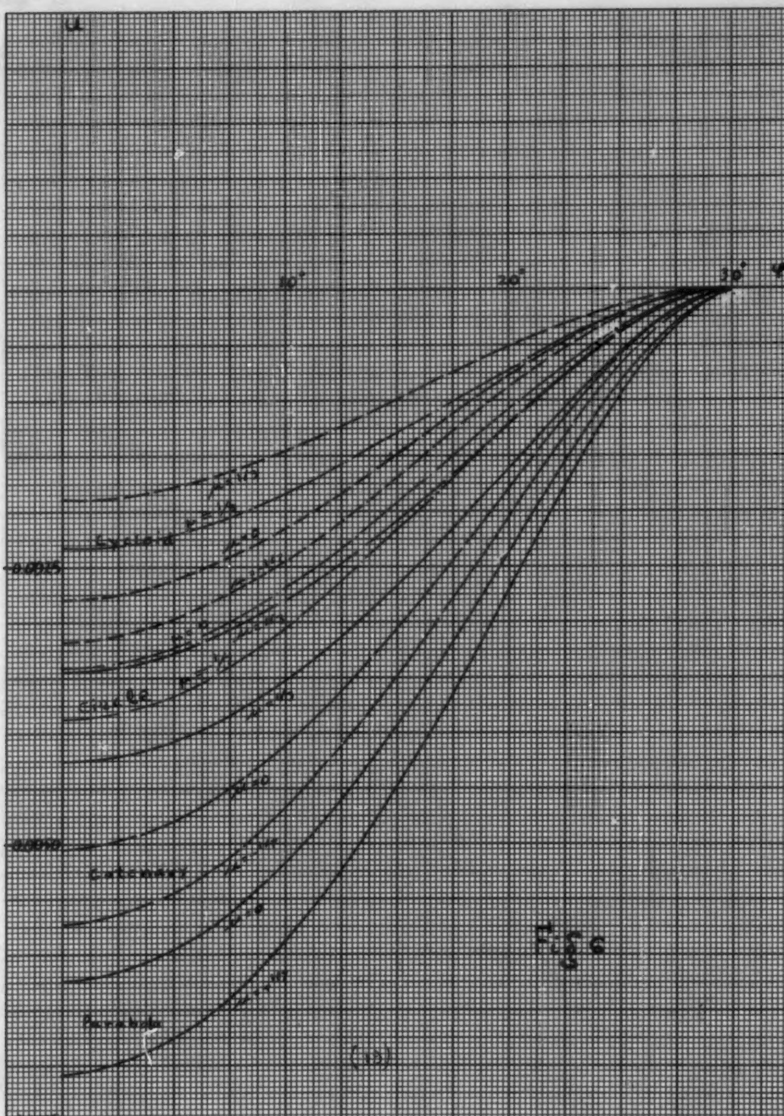
α
10°
20°
30°
φ
0.0025
0.0050
0.0075
Cycloid
Circle
Catenary
Parabola
Fig 6

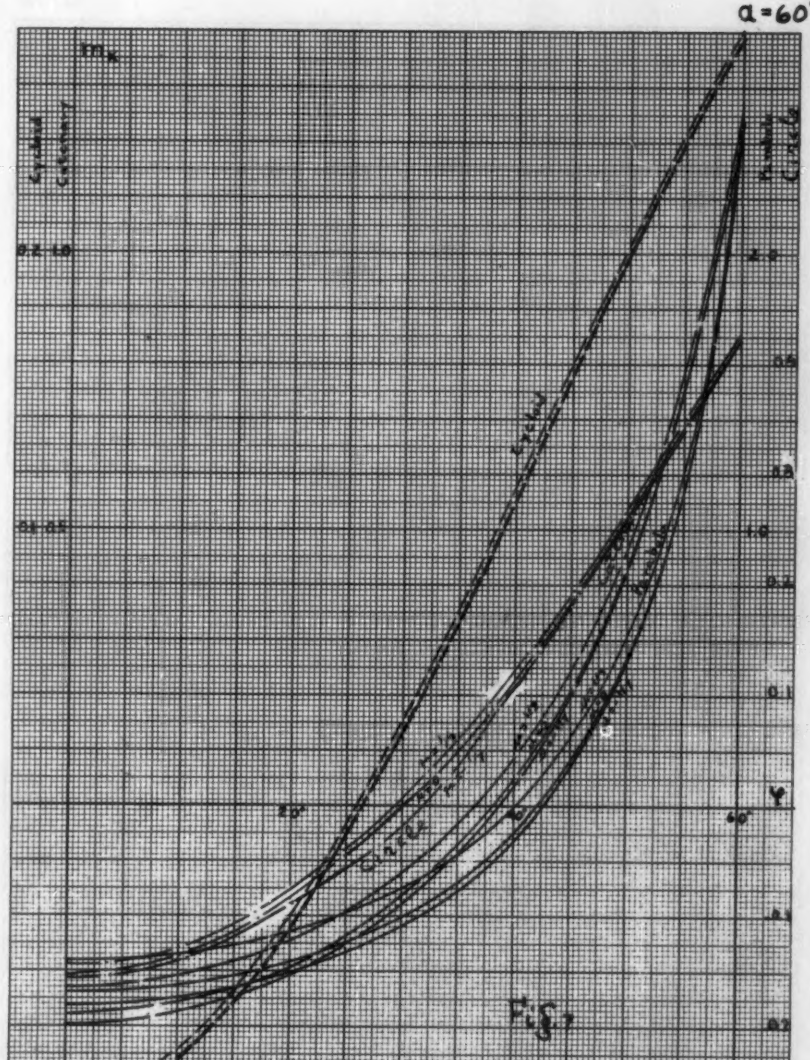
a=60°
m_x
Cycloid
Catenary
Parabola
Circle
Cycloid
Circle
Parabola
20°
40°
φ
Fig. 7
(20)

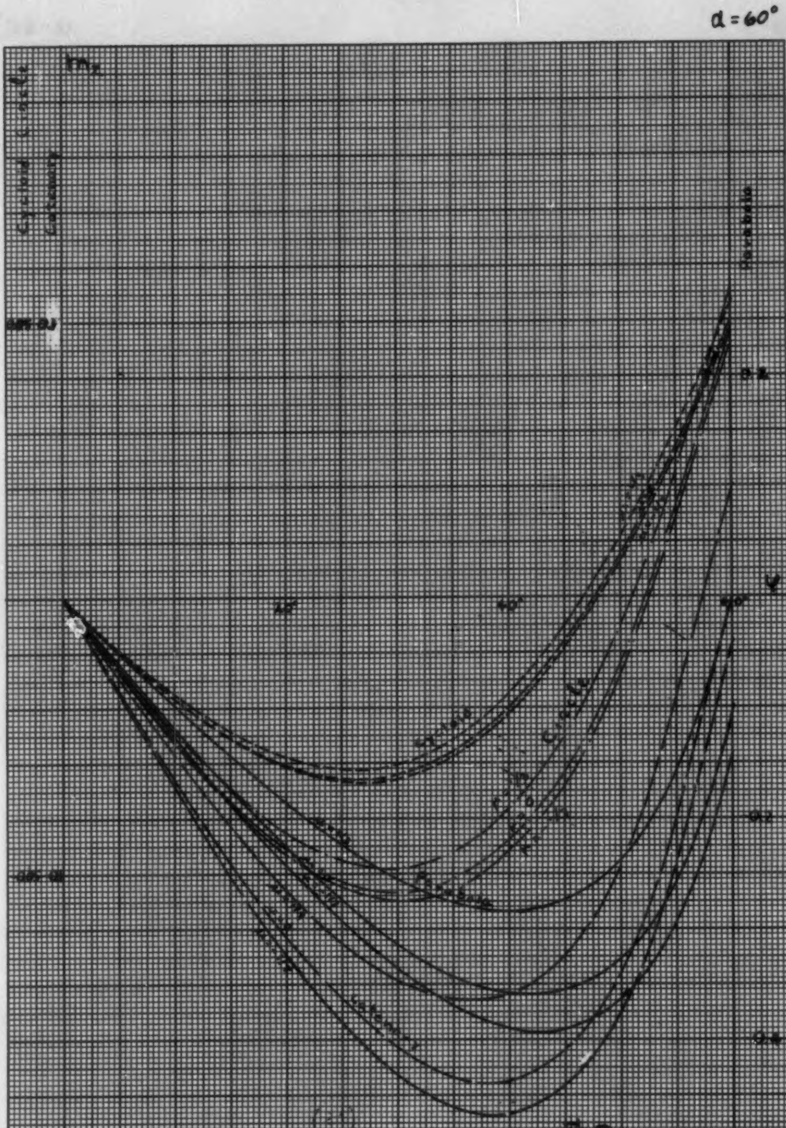

α = 60°
Cycloid
Circle
Catenary
Parabola
20°
40°
60°
Circle
Cycloid
Catenary
0.2

Fig. 8

a-60°

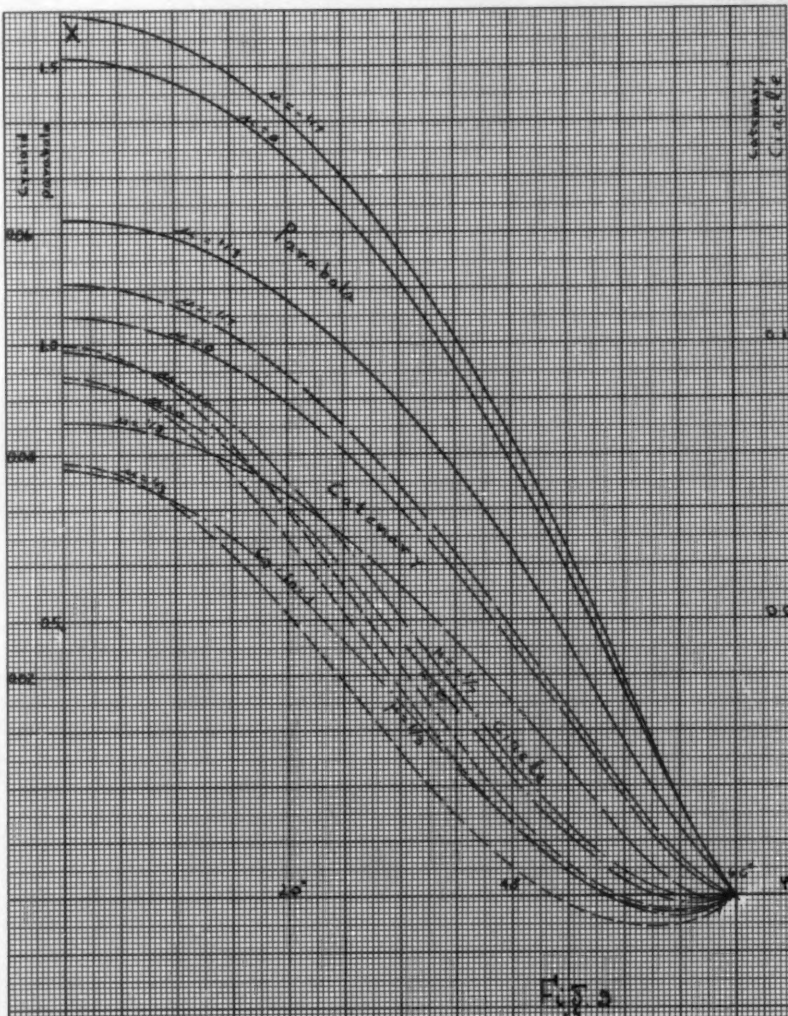

Fig. 2

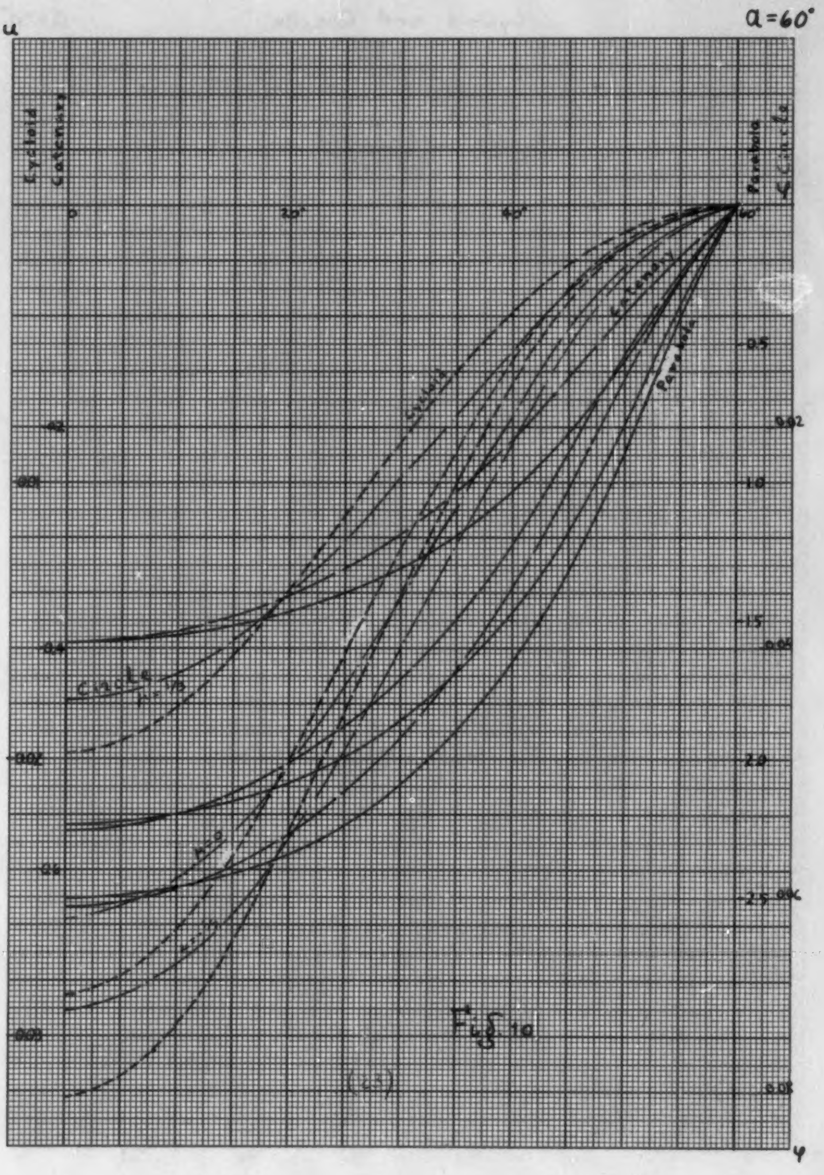
a=60°
u
Cycloid
Catenary
Parabola
Circle
0
20°
40°
60°
Cycloid
Catenary
Parabola
Circle
0.5
0.02
1.0
1.5
0.04
2.0
2.5
0.06
0.08
0.2
0.01
0.4
0.02
0.6
0.03
Fig. 10
y

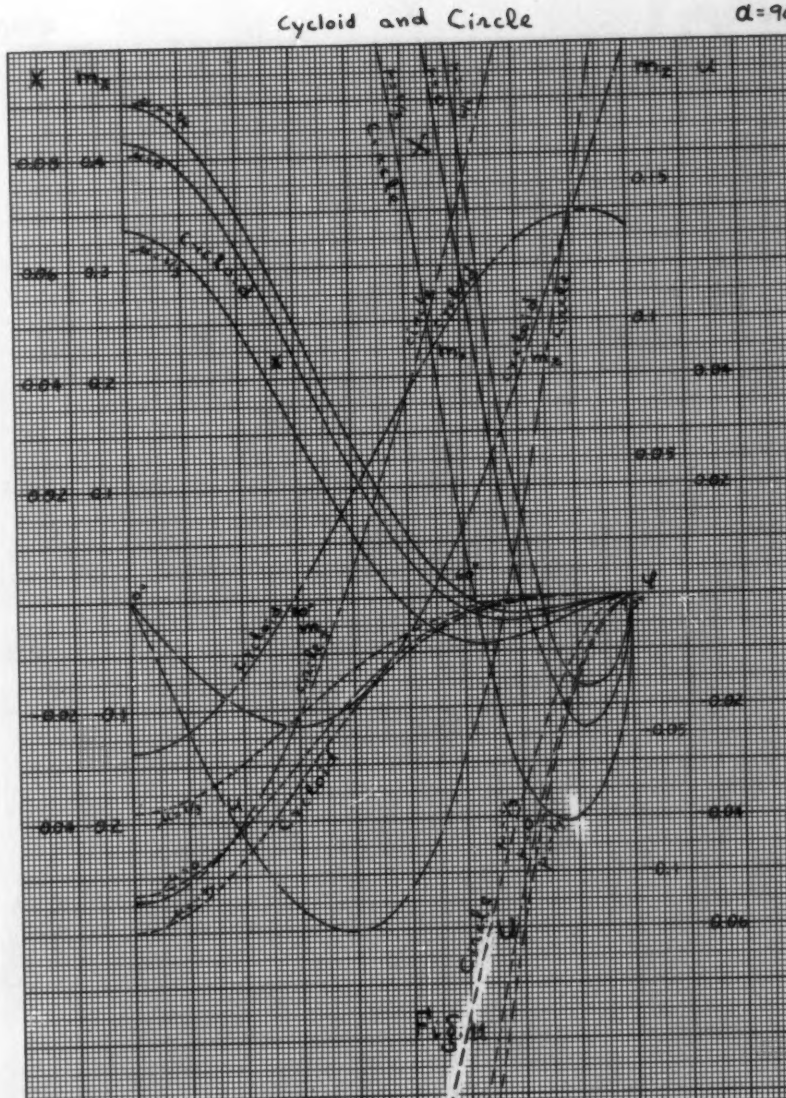

Cycloid and Circle
α=90°
X
m_x
m_z
α
0.08
0.4
0.06
0.3
0.04
0.2
0.02
0.1
0.15
0.1
0.05
Cycloid
Circle
Fig. 11

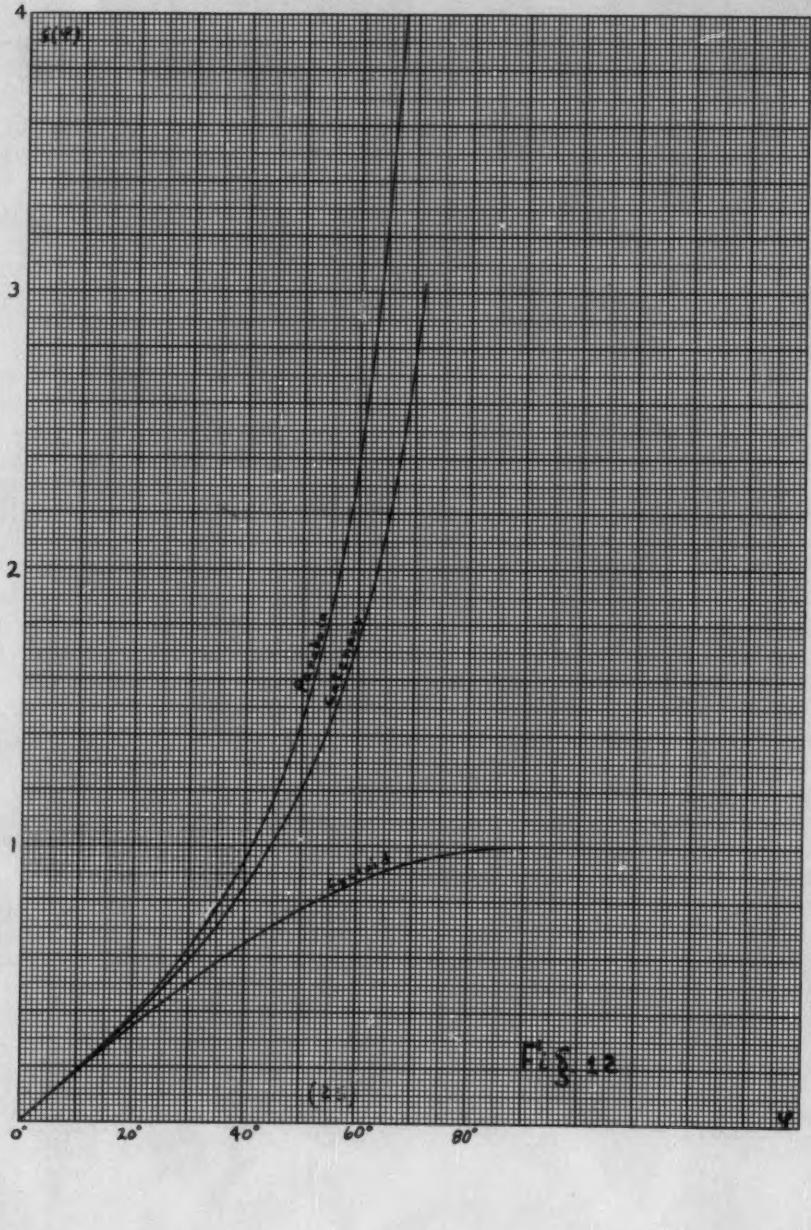

Fig. 12

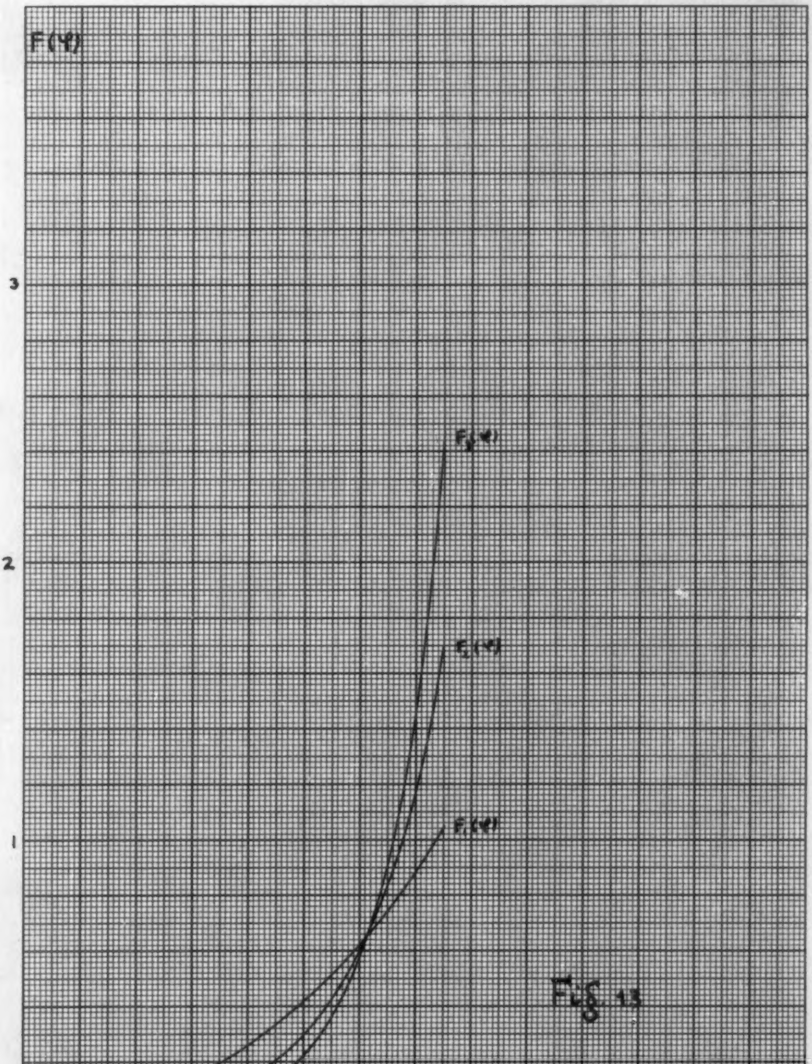

Fig. 13

JOURNAL

ENGINEERING MECHANICS DIVISION

Proceedings of the American Society of Civil Engineers

TABLE OF CONTENTS

DISCUSSION
(Proc. Paper 876)

A New Approach to Turbulent Boundary Layer Problems, by Donald Ross. (Proc. Paper 604) Prior discussion: Proc. Paper 776. Discussion closed.
by Donald Ross (Closure) 1

Failure of Plain Concrete under Combined Stresses, by Boris Bresler and Karl S. Pister (Proc. Paper 674) Prior discussion: Proc. Paper 776. Discussion closed.
by Henry J. Cowan, Boris Bresler and Karl S. Pister 7

Thick Rectangular Plates on an Elastic Foundation, by Daniel Frederick (Proc. Paper 818) Prior discussion: None. Discussion open until February 1, 1956. Corrections.
by Daniel Frederick 19

Note: Paper 876 is part of the copyrighted journal of the Engineering Mechanics Division of the American Society of Civil Engineers, Vol. 82, EM 1, January, 1956.

Discussion of "A NEW APPROACH TO TURBULENT BOUNDARY LAYER PROBLEMS"

by Donald Ross
(Proc. Paper 604)

DONALD ROSS.[1]—In attacking the problem of turbulent boundary layers, and in writing the subject paper, the writer has been primarily concerned with the case of boundary layers acted upon by adverse pressure gradients. For this reason, and also because several papers in the literature handle the subject successfully, that part of the original thesis dealing with equilibrium flows was omitted from the paper. However, in three discussions (see Proceedings Separate 776), Messrs. Baines, Robertson and Bauer have dwelled on this case and other readers may feel that it should receive specific attention.

For equilibrium boundary layers, there seems to be little question that equation 5 of the paper correctly represents the velocity distribution of the inner turbulent flow, although there may be some variation of the coefficients in equation 6. However, the velocity deficiency in the outer region may more properly be represented by the more general equation B proposed by Baines. The writer agrees with Baines and Bauer that a higher exponent is in better agreement with flat-plate data than the 3/2-power used by the writer. The writer chose the three-halves power because for flows having strong adverse pressure gradients the three-halves power law is a better fit than any other. Also, because the velocity deficiencies involved are so much greater near separation, the writer settled on the single formula giving the best fit for that type of flow and accepted the error typified by Bauer's Figure 14. It is not a serious discrepancy. In Figure 15 we may compare the writer's formula:

$$1 - \frac{u}{u_1} = 8.4 \sqrt{\frac{c_f}{2}} \left(1 - \frac{y}{\delta}\right)^{1.5}$$

with formulas of Baines and of Hama[2] and with the expression derived by von Kármán that the writer finds gives the best experimental fit. This

---

1. The Bell Telephone Laboratories, Inc., Whippany, N. J.
2. Hama, Francis R., "Boundary Layer Characteristics for Smooth and Rough Surfaces," Transactions, Society of Naval Architects and Marine Engineers, Vol. 62, 1954.

figure clearly shows that the differences between the writer's formula and Baines' are not great and that both give good average fits to experimental data. However, the true curve is not a power law, hence Bauer's result (Figure 14) that the value of D is not constant across the profile. Baines has incorporated the coefficient c_f in his formula for the outer velocity deficiency. This is valid for the constant pressure case, and the author confirms that D is proportional to $\sqrt{\frac{c_f}{2}}$ for flat plates. However, in general, for non-equilibrium boundary layers, i.e., boundary layers having profiles that change with distance, the local value of D is in no way dependent on the local value of c_f.

In reply to Baines, the writer believes that the methods developed in the paper can be extended to rough surfaces to the extent that these are understood. Thus, following Hama[2] and Clauser[3], we may write for the logarithmic inner-turbulent velocity profile:

$$\frac{u}{u_*} = A + B\log\frac{yu_*}{\nu} - \frac{\Delta U}{u_*}$$

where:

$$\frac{\Delta U}{u_*} = B\log\frac{ku_*}{\nu} + \text{const.}$$

in the fully developed roughness region, and is somewhat different in the transitional region. This factor is directly related to the increase of the surface friction that the roughness produces and its determination is discussed by Hama.[2] For a rough surface, equations 18 through 20 are applicable if u_{θ_e} is replaced by $(u_{\theta_e} + \Delta U)$. With this extension, most of the rest of the paper should be directly applicable to rough as well as smooth surfaces. As noted by Bauer, D will generally be larger for flows having rough walls.

Both Messrs. Baines and Robertson have pointed out that $\delta/\theta D$ is a function of c_f and/or R_θ for flat-plate conditions. In equation 15 of the paper, the relationship is only intended to be approximate and will be so corrected in the Transactions.

Another misprint has led Robertson to an erroneous analysis. Equation 20 should read:

$$\frac{u_1}{u_*} = \sqrt{\frac{2}{c_f}} \cong \frac{u_1}{u_{\theta e}}\left[0.7 + 5.0\log\left(R_\theta\frac{u_{\theta e}}{u_1}\right)\right],$$

without the plus sign that appears in the original printed version. Robertson's friction analysis based on that version must be in error and his simple conclusion does not hold.

Robertson's discussion of separation, on the other hand, should be valid, at least to the approximations made for his final equation. As Δx can be as great as 500 times θ_i, and as A can actually be much greater than he assumes, the term involving these two factors should not be dropped relative to f_i. In fact, the Sidney University experiments of Newman mentioned in his

3. Clauser, Francis H., "Turbulent Boundary Layers in Adverse Pressure Gradients," Journal of the Aeronautical Sciences, Vol. 21, 1954, p. 91.

discussion are an example where this term must be included. The curves shown in Robertson's Figure D are the limiting values for rapid decelerations.

In response to a request by Robertson, the accompanying table lists the sources of the experimental data and identifies the symbols used in Figures 9 and 11.

The writer wishes to thank the three discussers for their constructive comments, and he hopes that this closure sheds some light on the interesting questions that they have raised.

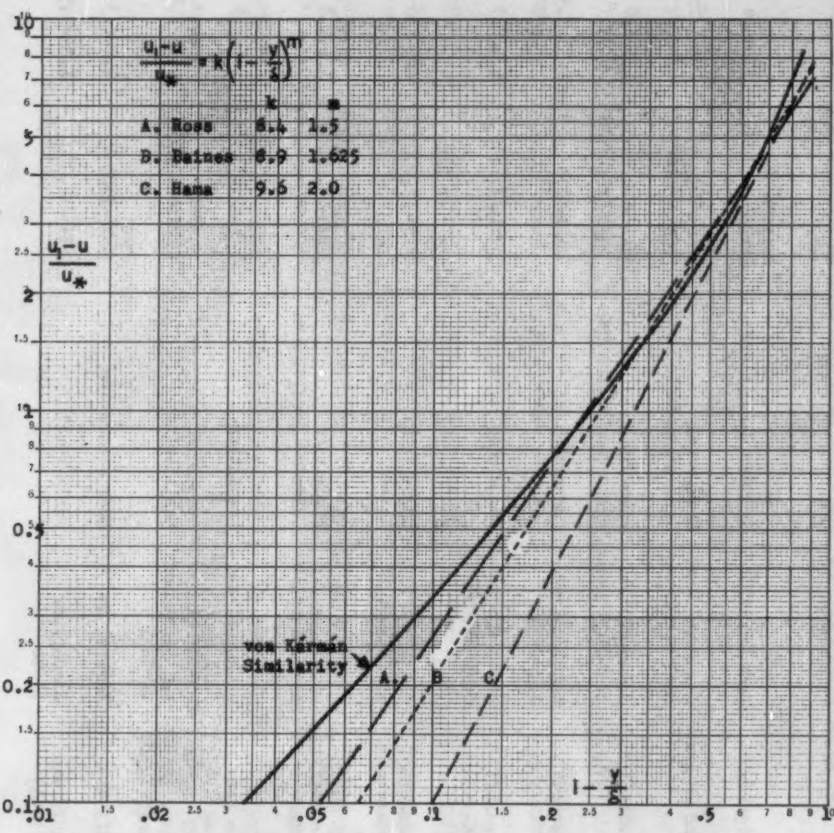

Figure 15 - Comparison of Outer Velocity Formulas for Flat Plates

TABLE I THE MAJOR EXPERIMENTS ON TWO-DIMENSIONAL TURBULENT BOUNDARY LAYERS SELECTED FOR THE PRESENT ANALYSIS

No.	Investigators	Test Object	Entrance Conditions	Approx. R_θ Range	H Range	No. of Stations	Symbols
1	Fage and Falkner (1930)	Joukowski airfoil at 0°	Transition	750-4000	1.4-1.55	7	⦸, ⊘
2	Gruschwitz (1931)	387 Airfoil at 12°	Transition	950-5400	1.4-1.8	6	◬
3	von Doenhoff (1940)	NACA 0012 at 0°	Transition	1200-8700	1.35-1.5	7	▽, △
4	von Doenhoff and Tetervin (1942)	66, 2-216 Airfoil at 10°	Transition	3200-13,200	1.5-2.3	6	<
5	von Doenhoff and Tetervin (1943)	65(216) - 222 Airfoil at 8°	Transition	1000-13,000	1.5-2.6	6	∨, ∧
6	von Doenhoff and Tetervin (1943)	65(216) - 222 Airfoil at 10°	Transition	3000-17,000	1.5-2.8	6	>
7	Preston and Sweeting (1943)	Joukowski airfoil at 0°, 6°	Transition	600-2350	1.5-1.8	8	⦶, ⊖
8	Schubauer and Klebanoff (1950)	NBS Simulated airfoil	Equilibrium	15,000-80,000	1.35-2.8	20	⊙
9	Newman (1950)	Airfoil at 9½°	Near separation	8400-9100	2.2-2.3	3	▽
10	Klebanoff and Diehl (1951)	Sand-paper plate	Fully rough	2000-15,000	1.35-1.9	12	X, +, Y

TABLE I - Continued

No.	Investigators	Test Object	Entrance Conditions	Approx. R_θ Range	H Range	No. of Stations	Symbols
11	Kehl(1943)	Channel AK III	Approx. Equilibrium	9000-29,000	1.2-1.45	14	◫
12	Kehl(1943)	Channel K3	Approx. Equilibrium	10,000-24,000	1.2-1.5	18	⊟
13	Kehl(1943)	Channel K7	Approx. Equilibrium	2,000-34,000	1.3-1.7	16	⧅ ⧄
14	Wieghardt and Tillmann(1944)	Channel IV	Transition at pressure dip	2000-90,000	1.25-1.7	16	▯
15	Hall(1946)	10°, Two-dimensional diffuser	Transition at pressure dip	700-12,000	1.25-2.15	12	⊡
16	Pierpont(1947)	Plate with suction slot	Various amounts of suction	1700-23,000	1.15-2.0	1	■
17	Newman(1949)	Airfoil with spoiler	Turbulent separation	18,000-52,000	1.6-3.6	8	▲ ▼
18	Bursnall and Loftin(1951)	66_3 - Airfoil at 0°	Laminar separation	1350-2000	1.25-1.65	6	●

Discussion of
"FAILURE OF PLAIN CONCRETE UNDER COMBINED STRESSES"

by Boris Bresler and Karl S. Pister
(Proc. Paper 674)

HENRY J. COWAN.[1]—The authors deserve to be congratulated on having reduced the problem of the failure of concrete under combined stresses to a criterion similar to that which has been found to govern the failure of ductile materials. This is a significant advance in the theory of the strength of materials. However, the authors dismiss too lightly some of the previous theories, notably Rankine's maximum stress theory, and Mohr's theory, of which Coulomb's internal friction theory is a special case.

While the mechanics of the failure of concrete are not fully known, it appears to be always initiated by the formation of very fine tension cracks, which are invisible or barely visible, but can, by careful measurement, be detected.(18, 19, 20) The ultimate failure of the concrete may, however, take two forms: a cleavage failure, which results in a clean fracture and is associated with the existence of high tensile stresses, and a crushing failure, which is accompanied by an appreciable formation of debris and is associated with the existence of high compressive stresses. This ultimate failure is immediately obvious and leads to the collapse of a plain concrete specimen, either instantly or after a short period of time has been allowed for the completion of the process of failure. In a reinforced concrete specimen a cleavage failure can be prevented by inserting suitable tension or shear reinforcement; however, the strength of the specimen thereafter is dependent on the strength of the steel.

It does not seem likely that a physical explanation of the process of failure in terms of atomic structure will be derived in the foreseeable future, since the structure of concrete, or even of cement, is vastly more complicated than that of a metal. A phenomenological explanation is necessarily only approximate, and it is desirable that it should be associated with clearly observed phenomena. Since in concrete there are two types of failure, it seems reasonable to use two criteria. The cleavage fracture is evidently dependent largely on the tensile strength of the cement. The aggregate plays, however, a great part in resisting compression, and the cement does not apparently alter its angle of internal friction appreciably at low triaxial pressures;(3,4)[2] the failure of concrete in compression is, therefore, not unlike that of a highly cohesive granular soil. In putting forward this physical explanation, the writer is conscious that it is an over-simplification, which will give way to a more precise interpretation when the structure of concrete is better understood.

The above considerations led the writer(21) to adopt the dual criterion of failure referred to by the authors. The maximum stress theory has been used on numerous occasions to account for the cleavage, or tension, fracture

1. Prof. of Architectural Science, Univ. of Sydney, Australia.
2. Authors' reference, Separate No. 674.

of brittle materials, including concrete. Mohr's theory, using a curved envelope, has similarly accounted for the crushing failure of concrete. The first attempt at a unified criterion of failure appears to have been made by Leon,[5] using Mohr's theory with a continuous curved envelope, crossing the σ - axis on the tension side. This is represented by the curved line ABA in fig. 8. Leon explained that a Mohr circle touching the envelope at B corresponded to a cleavage failure, and Mohr circles touching the envelope elsewhere corresponded to compression failures. The curved envelope is, however, an unsatisfactory criterion for the concrete designer, since it cannot be expressed in simple mathematical terms, and varies for different types of concrete. This difficulty is overcome by using a vertical limiting line DBD for the cleavage failure (Rankine's maximum stress theory), and two limiting lines CC for the crushing failure. In the range of low triaxial stresses straight limiting lines may be used with sufficient accuracy (Coulomb's internal friction theory). Both the cleavage and the crushing failure can therefore be expressed in terms of the principal stresses: a constant maximum tensile stress, and a maximum compressive stress which varies linearly with the minor (tensile of compressive) principal stress. The dual criterion of failure can be readily applied to reinforced and prestressed concrete design. The linear relationship is sufficiently accurate for building construction; it does not apply to structures with high triaxial stresses, e.g., large concrete dams.

Cowan and Armstrong[22][3] have checked this criterion in an investigation on reinforced and prestressed concrete beams under combined bending and torsion, and have suggested a procedure for structural design. The criterion has also been checked with the results of two earlier investigations on concrete and reinforced concrete in combined bending and torsion.[23,24] In all cases, generally, good agreement with the experimental data was found. The only significant difference between theory and experiment occurred at the transition from primary torsion (cleavage) to primary bending (crushing) failure, since the dual criterion produces a sharp corner in the limiting line, whereas the experimental results follow a more gradual curve; however, this divergence is not of practical significance.

A three dimensional representation in terms of the principal stresses of the criteria used by Bresler and Pister, Leon, and Cowan and Armstrong (Figs. 9 - 11) shows that the difference between them is due mainly to the effect of the intermediate principal stress: they are not as dissimilar as they appear to be when expressed in mathematical terms, and, indeed, this is borne out by a comparison with the experimental data. The intermediate principal stress does not play a significant part in a large range of combined stress problems, notably those met in the design of reinforced and prestressed concrete structures. Ease of application is, on the other hand, of prime importance in these problems. The writer therefore feels that the authors have been a little harsh in their discussion of some of the previous theories. This comment is not, however, intended to detract from the important contribution which the authors have made to the theory of fracture of concrete.

---

3. The full results of this investigation were published after the Authors wrote their paper.

REFERENCES

18. Berg, O. Y., "The Problem of the Strength and Plasticity of Concrete" (in Russian), Doklady Akademii Nauk S.S.R., Vol. 7, pp. 617-620 (1950); translated as Road Research Library Communication No. 165, London 1951.

19. Jones, R., "A Method of Studying the Formation of Cracks in a Material Subjected to Stress," Brit. J. Appl. Phys., Vol. 3, pp. 229-232 (1952).

20. Blakey, F. A., and Beresford D., "Tensile Strains in Concrete," C.S.I.R.O., Div., Bldg. Res., Rep. No. C2.2-1 and 2, Melbourne 1953 and 1955.

21. Cowan, H. J., "Strength of Reinforced Concrete under the Action of Combined Stresses, and the Representation of the Criterion of Failure by a Space Model," Nature, Vol. 169, p. 663 (1952).

22. Cowan, H. J., and Armstrong, S., "Experiments on the Strength of Reinforced and Prestressed Concrete Beams and of Concrete-Encased Steel Joists in Combined Bending and Torsion," Mag. Conc. Res., Vol. 7, pp. 3-20, (1955).

23. Nylander, H., "Vridning och vridningsinspanning vid betongkonstruktioner," Statens Kommitté för Byggnadsforskning, Meddelanden No. 3, Stockholm 1945.

24. Fisher, D., "The Strength of Concrete in Combined Bending and Torsion," University of London, Thesis for the Degree of Ph.D., (unpublished), 1950.

Note: Discussion of Proc. Paper 674 is continued by Bresler and Pister on page 13.

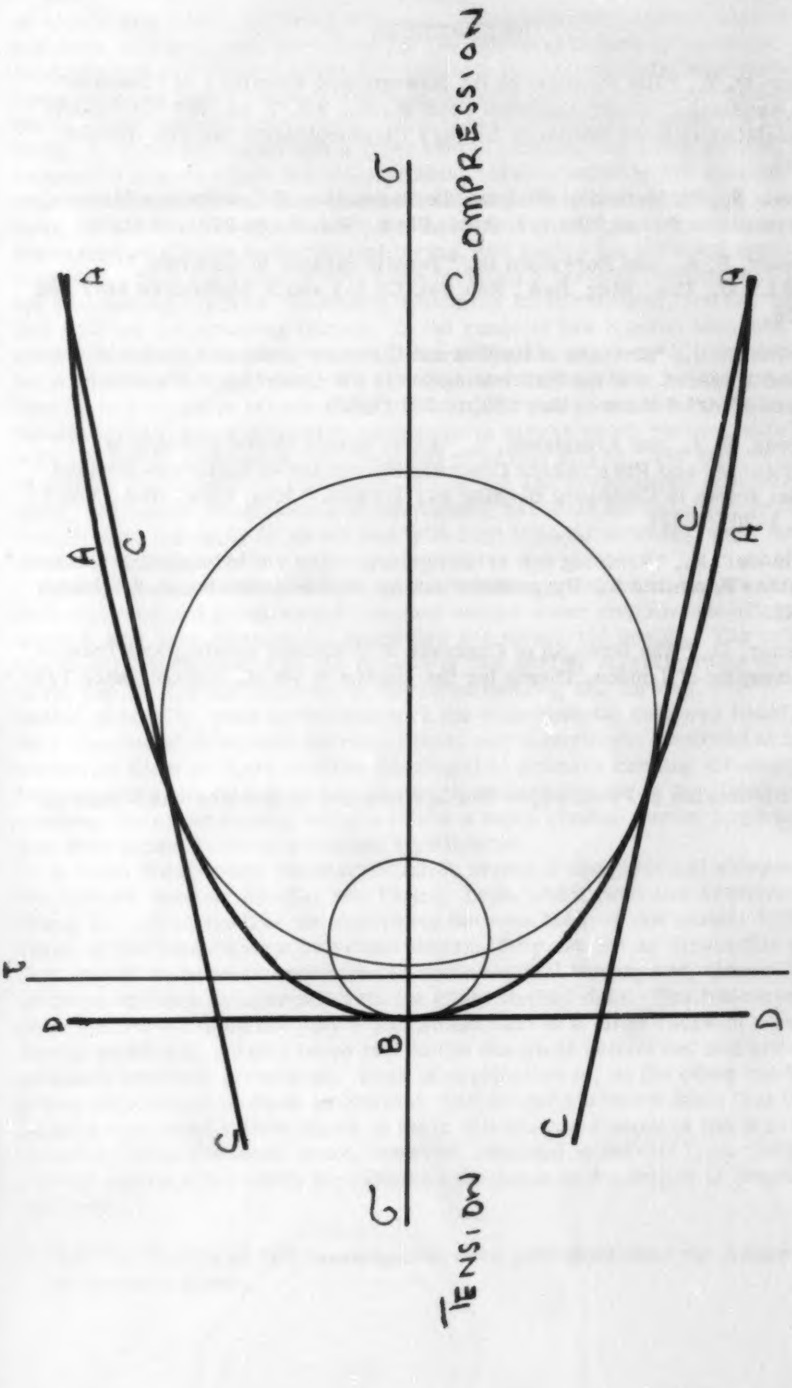

Fig. 8—Mohr Circle Representation of Leon's and Cowan's Failure Criteria.

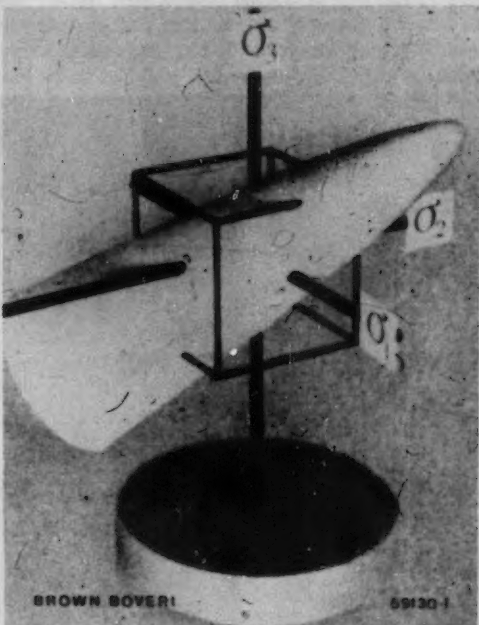

Fig. 9—Bresler's and Pister's Failure Criterion. (σ_1 σ_2, and σ_3 denote the principal stresses). (From Brown Boveri Review, August 1944)

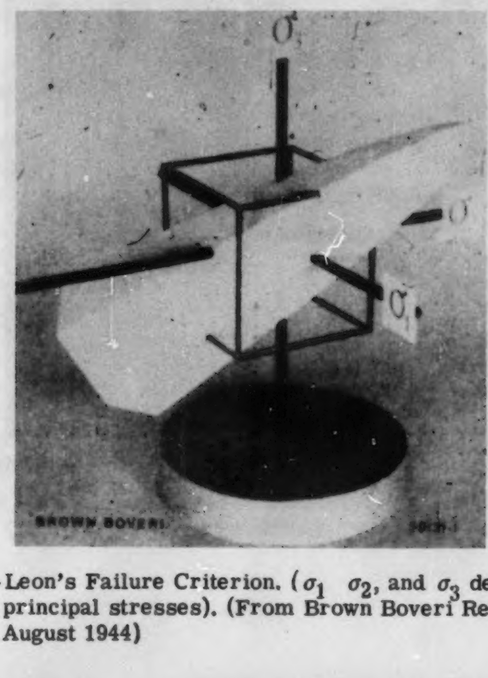

Fig. 10—Leon's Failure Criterion. (σ_1 σ_2, and σ_3 denote the principal stresses). (From Brown Boveri Review, August 1944)

Magazine of Concrete Research: December 1953

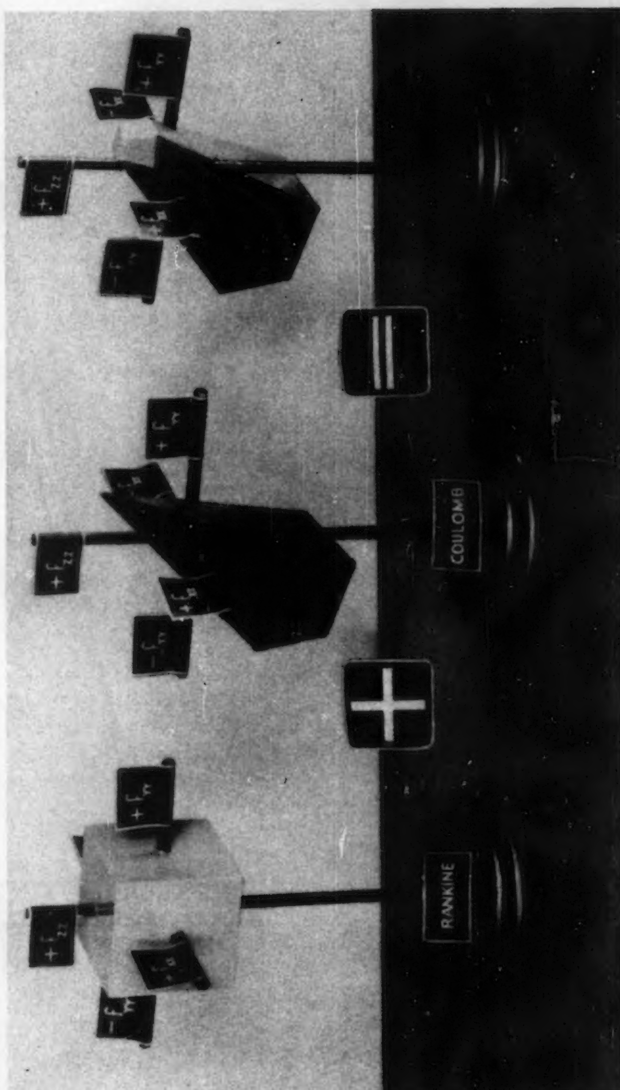

Fig. 11—Cowan's Failure Criterion. The dual criterion is obtained by combining Rankine's maximum stress criterion with Coulomb's internal friction criterion. (f_{xx}, f_{yy}, and f_{zz} denote the principal stresses). (From Magazine of Concrete Research, December 1953).

BORIS BRESLER,[1] A.M. ASCE, and KARL S. PISTER,[2] J.M. ASCE.—The comments of the discussers fall into two main categories: (1) utility of proposed failure criteria for design, and (2) physical interpretation of failure criteria and mechanism of failure. Whether one form of failure criterion is superior to another is largely a matter of the use intended for it. The interaction formula proposed by Professor Smith is useful in design but is entirely empirical. Professor Cowan proposes dual criteria which are somewhat more rational but are more difficult of application. Neither criterion is applicable to triaxial states of stress. The writers' criterion, although not directly applicable to design, may be useful for correlating biaxial and the triaxial tests and for furthering the understanding of the physical mechanism of failure. It was the authors' opinion that once a valid criterion is established, simplications suitable for design can be derived. For example, in the case of shearing stress τ combined with compressive stress σ equation (6) leads to the following definition of shearing strength of concrete:

$$\frac{\tau}{f_c'} = 0.10 \left[0.89 + 8.9 \left(\frac{\sigma}{f_c'}\right) - 10.8 \left(\frac{\sigma}{f_c'}\right)^2 \right]^{\frac{1}{2}}$$

The writers are grateful to Mr. Rice for pointing out the agreement between the writers' work and Professor Smith's experiments. It should be noted, however, that the type of loading used in Professor Smith's experiments produced a stress field which is difficult to analyze by elementary methods; therefore, the agreement obtained seems rather fortuitous.

In formulating the failure law in terms of octahedral stress the writers were guided by several considerations:

(1) The failure criterion in the form of Eq. (4), $\tau_o = F(\sigma_o)$, accounts for the effect of the intermediate principal stress, σ_2, and thus is a natural generalization of the Mohr theory of failure which neglects the effect of σ_2. Furthermore, use of octahedral stresses allows plotting both biaxial and triaxial states of stress in one plane. A comparison of three possible forms of representation of a failure criterion is shown in Fig. 8. Figure 8a shows Mohr's failure theory in terms of normal and shearing stresses; Figure 8b shows a failure criterion for brittle materials in terms of principal stresses; Fig. 8c shows a similar criterion in terms of octahedral stresses. Radial lines define some of the possible states of stress, and it is seen that only the octahedral form permits plotting triaxial states of stress in one plane.

(2) Octahedral stresses have physical interpretations which may lead to a better understanding of the mechanism of failure in concrete. The normal octahedral stress is the mean normal stress, and the shearing octahedral stress is proportional to the root mean shear stress at a point. Thus Eq. (4) suggests that the failure mechanism may be defined in terms of the mean shearing and normal stresses at a point. Another possible interpretation of octahedral stresses, as pointed out by Messrs. Blakey and Beresford, is related to the elastic strain energy and the volumetric strain. It seems doubtful that elastic strain energy concepts based on homogeneous materials with relatively constant values of elastic modulus and Poisson's ratio would be

---

1. Associate Prof. of Civ. Eng., Univ. of California, Berkeley, Calif.
2. Asst. Prof. of Civ. Eng., Univ. of California, Berkeley, Calif.

applicable to concrete. This view is supported by the presence in Blakey and Beresford's equations of odd terms, involving the second stress invariant I_2, which apparently have no simple physical interpretations. A valid adaption of strain energy criteria to concrete must be based on a physical concept of the mechanism of deformation and failure.

(3) Within the range of states of stress considered by the writers, the octahedral stress criterion has a further advantage in its simplicity of form, resulting in a simple linear equation, the writers' Eq. 6.

Professor Cowan's linear criterion of failure, differentiating between cleavage and crushing failures, is shown in Fig. 9 by dashed lines. Whether or not the transition from a pure cleavage to a shear fracture in concrete is gradual or abrupt seems to be a matter that is still unsettled. The parbolic envelope assumed by Leon for brittle materials provides a gradual transition from cleavage to shear fracture. For biaxial state of stress, $\sigma_2 = 0$, Equation (6) may be rewritten in terms of principal stresses by substituting Eq. (5) into Eq. (6). This leads to a quadratic expression involving σ_1, σ_3 σ_c, and the experimental constants. The equation may be simplified by rotation of the σ_1, σ_3 coordinate axes through a counter-clockwise angle of 45°. If the new coordinate axes are denoted by $\bar{\sigma}_1$, $\bar{\sigma}_3$ the following equation results:

$$\frac{\left(\dfrac{\bar{\sigma}_1}{\sigma_c} + 0.257\right)^2}{0.0251} - \frac{\left(\dfrac{\bar{\sigma}_3}{\sigma_c}\right)^2}{0.0138} = 1.00$$

where

$$\sigma_1 = \frac{1}{\sqrt{2}}\left(\bar{\sigma}_1 - \bar{\sigma}_3\right)$$

$$\sigma_3 = \frac{1}{\sqrt{2}}\left(\bar{\sigma}_1 + \bar{\sigma}_3\right)$$

This is the equation of an hyperbola in the pincipal stress plane, Fig. 9, and is similar to Fig. A by Messrs. Blakey and Beresford. It can be seen that Leon's theory and the octahedral theory propose a single criterion applicable to both cleavage and shear failures, while Cowan proposes two distinct criteria with an abrupt transition between them. Aside from this aspect of their interpretation, the agreement between Cowan's theory and that of the writers appears to be good.

It must be understood that the proposed linear octahedral theory as yet is untested for states of stress in which the mean stress is tensile. (States of stress to the left of the τ_0 axis in Fig. 8c). It may well be that some modifications in the assumed linear curve may be necessary. In order to test the validity of Eq. (6) beyond the range of the writers' experimental data it may be of interest to extrapolate the straight line as shown in Fig. 10 and evaluate the strengths for various states of stress on this basis. The uniaxial tensile strength based on this assumption is $0.10\sigma_c$ or $0.087\, f'_c$. The torsional strength, or biaxial, equal tension-compression strength, is $0.10\sigma_c$, i.e. very nearly equal to tension. The biaxial, equal tension-tension strength is $0.07\,\sigma_c$ or $0.061\, f'_c$, i.e., seventy per cent of the uniaxial tensile strength. These values appear to be reasonable.

Messrs. Blakey and Beresford define failure as formation of microcracks at loads below the ultimate. The writers believe that the formation of microcracks is an important factor in the mechanism of failure, but that the extent to which these cracks jeopardize the load carrying capacity of concrete has not been definitely established. The work done by the discussers indicates ratios of cracking to an ultimate load varying from 0.43 to 0.80. Until the mechanism of failure in concrete is better understood the definition of failure shall remain arbitrary.

The writers agree with Messrs. Blakey and Beresford that a complete study of strain distribution in the hollow cylinders would have been of interest. This study was not included by the writers primarily because interpretation of strain measurements in concrete is hazardous. Only surface strains can be measured without disturbing the internal structure of the material. Thus, the interpretation that deviation from linearity of load strain curve is evidence of microcracking is strictly applicable to the surface material only. The fact that surface cracking occurs at small fractions of the ultimate load seems to indicate that propagation of surface cracking with increase in load is slow, and that considerable load resisting capacity is developed after initial cracking.

In conclusion the writers wish to convey their sincere appreciation for the valuable comments of the discussers.

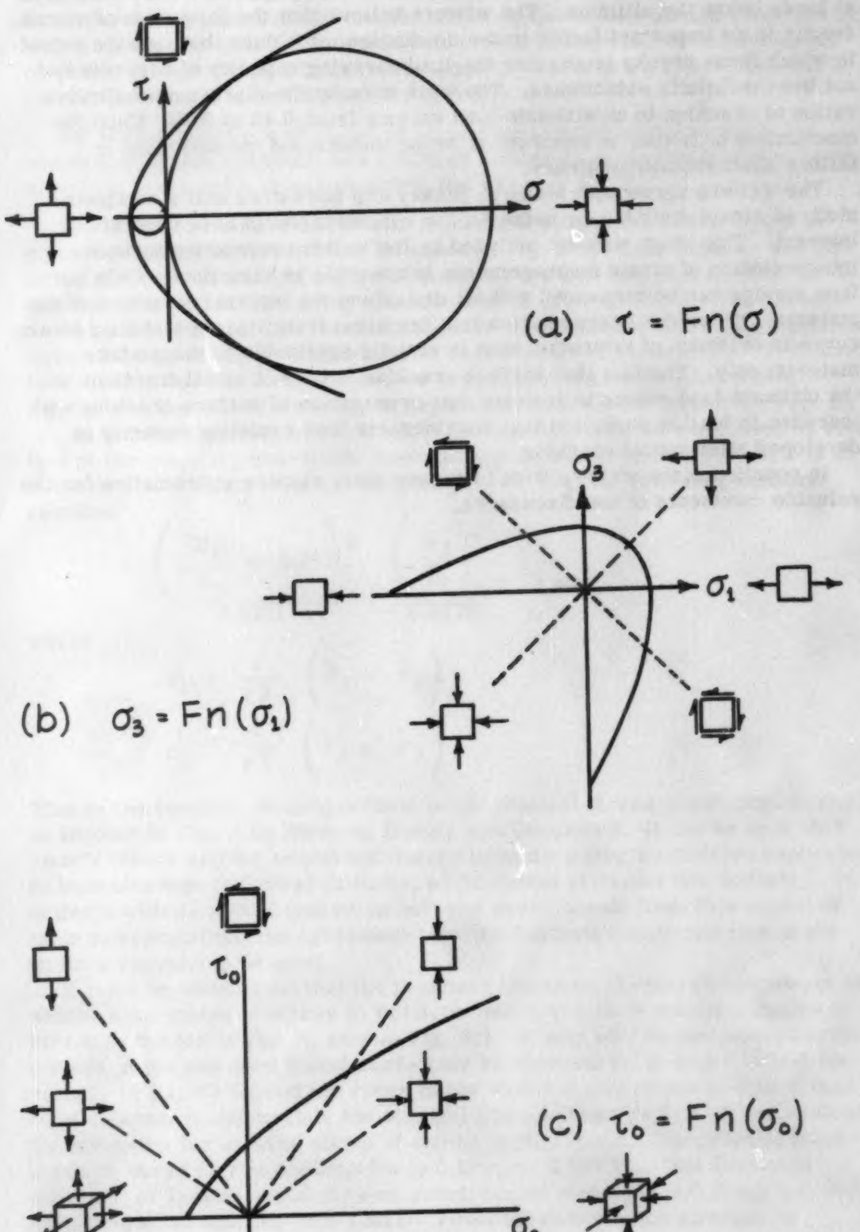

FIG. 8

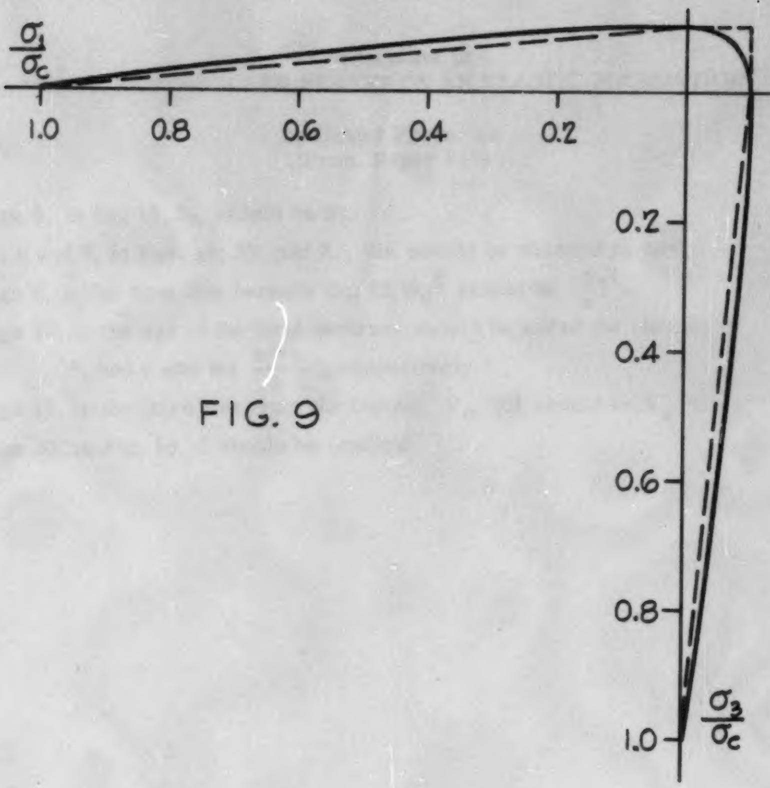
$\frac{\sigma_1}{\sigma_c}$
1.0
0.8
0.6
0.4
0.2
0.2
0.4
0.6
0.8
1.0
$\frac{\sigma_3}{\sigma_c}$

FIG. 9

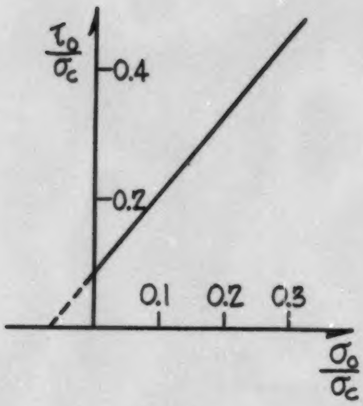
$\frac{\tau_o}{\sigma_c}$
0.4
0.2
0.1
0.2
0.3
$\frac{\sigma_o}{\sigma_c}$

FIG. 10

Corrections to
"THICK RECTANGULAR PLATES ON AN ELASTIC FOUNDATION"

by Daniel Frederick
(Proc. Paper 818)

Page 8, in Eq. 19, b_n should be w_n.

Pp. 8 and 9, in Eqs. 19, 22, and 23, sin should be changed to cos.

Page 9, in the first line beneath Eq. 23, $\alpha_n{}^2$ should be $(\frac{n}{a})^2$.

Page 10, at the end of the first sentence should be added the phrase:

", and y and sin $\frac{n\pi x}{a}$, respectively."

Page 11, in the third line from the bottom, V_α (0) should be V_x (0).

Page 20, in Fig. 5d, C should be omitted.

[illegible]

"THICK RECTANGULAR PLATES ON AN ELASTIC FOUNDATION"

[illegible]

Page 5, in eq. (2), [illegible] should be [illegible]

Figs 8 and 9, in [illegible] should be changed to [illegible]

Page 9, in the first line beneath eq. [illegible]

Page 10, at the end of the first paragraph, [illegible]

[illegible]

Page 11, in the [illegible]

Page 21, in Fig. 14, [illegible] should be omitted.